Global foundations for reducing nutrient enrichment and oxygen depletion from land based pollution, in support of the

Global Nutrient Cycle

Report 2
Nutrient release in global coastal marine ecosystems, and modeling of impacts in relation to coastal conditions

Prepared by Utrecht University, Washington State University, IOC-UNESCO

Component B: Doc: B2/B3-1

Partners:

November 2015

About the GEF-Global Nutrient Cycle Project

Project objective: to provide the foundations (including partnerships, information, tools and policy mechanisms) for governments and other stakeholders to initiate comprehensive, effective and sustained programmes addressing nutrient over-enrichment and oxygen depletion from land based pollution of coastal waters in Large Marine Ecosystems.

Core project outcomes and outputs:

- the development and application of quantitative modeling approaches: to estimate and map present day contributions of different watershed based nutrient sources to coastal nutrient loading and their effects; to indicate when nutrient over-enrichment problem areas are likely to occur; and to estimate the magnitude of expected effects of further nutrient loading on coastal systems under a range of scenarios
- the systematic analysis of available scientific, technological and policy options for managing nutrient over-enrichment impacts in the coastal zone from key nutrient source sectors such as agriculture, wastewater and aquaculture, and their bringing together an overall Policy Tool Box
- the application of the modeling analysis to assess the likely impact and overall cost effectiveness of the various policy options etc brought together in the Tool Box, so that resource managers have a means to determine which investments and decisions they can better make in addressing root causes of coastal over-enrichment through nutrient reduction strategies
- the application of this approach in the Manila Bay watershed with a view to helping deliver the key tangible outcome of the project – the development of stakeholder owned, cost-effective and policy relevant nutrient reduction strategies (containing relevant stress reduction and environmental quality indicators), which can be mainstreamed into broader planning
- a fully established global partnership on nutrient management to provide a necessary stimulus and framework for the effective development, replication, up-scaling and sharing of these key outcomes.

Project partners:

- Chilika Development Authority
- Energy Centre of the Netherlands
- Global Environment Technology Foundation
- Government of India - Lake Chilika Development Authority
- Government of the Netherlands
- Government of the Philippines
- Government of the United States
- Intergovernmental Oceanographic Commission of UNESCO
- International Nitrogen Initiative
- Laguna Lake Development Authority
- Partnerships in Environmental Management for the Seas of East Asia
- Scientific Committee on Problems of the Environment
- University of Maryland
- University of the Philippines
- University of Utrecht
- Washington State University
- World Resources Institute

Implementing Agency: United Nations Environment Programme
Executing Agency: UNEP- Global Programme of Action for the Protection of the Marine Environment from Land-Based Activities (GPA)

Nutrient release in global coastal marine ecosystems, and modeling of impacts (hypoxia, harmful algal blooms and fisheries) in relation to coastal conditions

Report on component B2 and B3 of the Global Environment Facility (GEF), United Nations Environment Programme (UNEP), Intergovernmental Oceanographic Commission of the UNESCO (IOC/UNESCO) project "Global foundations for reducing nutrient enrichment and oxygen depletion from land based pollution, in support of Global Nutrient Cycle"

27 November 2015

A.F. Bouwman[a], A.H.W. Beusen[b],

Department of Earth Sciences–Geochemistry, Faculty of Geosciences, Utrecht University, Utrecht, The Netherlands

J.A.Harrison[c], D.C. Reed[d]

School of Earth and Environmental Sciences, Washington State University, Vancouver, Washington, USA.

[a] a.f.bouwman@uu.nl

[b] a.h.w.beusen@uu.nl

[c] john_harrison@wsu.edu

[d] dan.reed @wsu.edu

Table of contents

1. Introduction

Component B of the project GEF/UNEP/IOC project "Global foundations for reducing nutrient enrichment and oxygen depletion from land based pollution, in support of Global Nutrient Cycle" addresses the need for more quantitative nutrient analysis, particularly in developing countries, and the exchange of information on this. In an innovative way, the component aims at improved predictive capability and use of tools, guidelines and modeling outputs by relevant stakeholders in order to estimate the magnitude of contributions from various nutrient sources within watersheds and quantitatively analyze relationships between nutrient sources and coastal impacts.

The work in component B focuses on two different scales, i.e. global and regional/local. During the project preparation phase it was agreed to use the Global NEWS databases and models developed in the UNESCO-IOC project Global NEWS as a basis for the planned work at the global scale. Manila Bay was selected as the demonstration region for the project. For the Manila Bay region more detailed data and models are needed than for the global-scale work.

This report describes the global scale data and analyses done in component B2 and B3. Below the work plan for the global scale database development and nutrient impact modeling is summarized; the chapters describing the results of the various tasks are indicated. All databases collected, data compilations, and figures will be made available through the GPNM website (http://www.nutrientchallenge.org/filebrowser).

Global database development on coastal nutrient loading and environmental conditions

Chapter 2. Global-NEWS data for river nutrient (nitrogen, N; phosphorus, P; Silicon, Si) export of dissolved (D) inorganic (I) nutrients (DIN, DIP, DSi), dissolved organic (DON, DOP) and particulate (PN, PP), as well as suspended solids, as published in the recent Global NEWS special issue of Global Biogeochemical Cycles (Seitzinger et al., 2010a). This database includes estimates of nutrient export by individual form for the years 1970, 2000, and scenario runs using four Millennium Ecosystem Assessment scenarios for 2030 and 2050.The datasets include all the background data used to drive the Global NEWS models, such as atmospheric deposition estimates, fertilizer inputs, manure inputs, and N fixation inputs, as well as indicators like the Index for Coastal Eutrophication (ICEP). These datasets have been available, but have also benefitted greatly from additional work including an effort to split DIN into reduced (ammonium, NH_4^+) and oxidized nitrogen (Nitrate, NO_3^-). This is necessary for better describing the impact of nutrient forms on the development of harmful algal blooms of some specific algae.

Chapter 3. Nutrient release and transformations from aquaculture. This work was performed in the framework of the SCOR-LOICZ work group 132 on harmful algal blooms, and is also readily available for use in this project. The data include model-based estimates of nutrient inputs and outputs for aquatic plants (seaweed), crustaceans, molluscs and finfish. Crustaceans and finfish in marine environments are generally fed various feedstuffs, while molluscs generally filter suspended material (algae, sediment, etc.) and transform this to pseudofaeces, faeces and dissolved nutrients. However, in the published work of the SCOR work group country-scale estimates are available, and application at the scale of coastal marine ecosystems will require additional work. This additional work includes improved allocation within the coastal seas of each country, and a split of the release of dissolved nutrients into specific nutrient species (ammonium, urea, nitrate).

Chapter 4. Global database development with data on coastal conditions, non land-based nutrient sources, as well as coastal effects collected from existing sources. This task involves the collection of required data needed to describe the physical and environmental conditions in coastal marine ecosystems worldwide. Basic to this work is the coastal typology developed by Dürr et al. (2011). In addition, this activity aims at collecting information on coastal upwelling, stratification, and productivity, as well as other necessary ancillary data. Major upwelling regions have been identified using globally available databases. We have developed a new method to estimate rates of coastal nutrient supply due to upwelling because such an estimate was previously unavailable. Stratification is another important process determining the development of algal blooms and hypoxia, so we have also developed indicators of stratification at the global scale.

Chlorophyll *a* concentration and primary productivity are two key factors with the potential to affect risk of hypoxia and harmful algal blooms. Global satellite data were used to estimate chlorophyll a concentrations and primary productivity and to test for relationships between chlorophyll *a*, primary production and occurrence of hypoxia.

Observed impacts

Chapter 5. Occurrences of hypoxia and harmful algal blooms. This task involves the collection of available and published data on observed hypoxia events and harmful algal blooms (HABs). Data sources included Diaz and Rosenberg (2008) for hypoxia, the SCOR-LOICZ work group 132 on harmful algal blooms, IOC database (HAEDAT) and other data.

Impacts on fisheries were analyzed by collecting available data from World Fish Centre, FAO, OSPAR and other data sources, and model output from regions where Ecopath and EcoSim models, a widely used ecological modeling software developed

at University of British Columbia's Fishery Centre in Canada. So far these systems include > 70 coastal systems worldwide. We have explored using these systems to develop relationships between fishery production and potential controlling variables such as nutrient inputs and hypoxia. Eventually, such relationships can be used to support estimates of anthropogenic impacts on fisheries at the global scale.

Nutrient impact modeling for global and local to regional nutrient source impact analysis

Chapter 6. Enhance predictive capability of models with respect to nutrient sources, loads, and coastal impacts. Data from the SCOR/LOICZ HAB work group was used in conjunction with information about HAB risk indicators such as the ICEP indicator to develop quantitative models predicting the probability of HAB occurrence as a function of nutrient loads and sources. A coastal filter model was explored but ultimately we decided not to use this model due to uncertainty associated with coastal residence time approach. Instead, we developed and applied a new, one-dimensional model for use at the level of coastal segments with their corresponding river catchments (COSCAT). This model and its output is briefly described in this chapter.

Chapter 7. Assessment of effects of nutrient loading in coastal marine ecosystems. Relationships developed in Chapter 6 have been used to develop maps indicating where hypoxia and HABs are likely to occur under current and recent historic conditions. This Chapter will also analyze maps of past, current and future contributions of different nutrient sources, forms and ratios in watersheds to coastal effects. Maps will be analyzed to identify regions likely to experience rapid increases in nutrient-related problems over the next several decades. Primary sources of nutrients to these coastal regions will also be estimated as such information is necessary to support attempts at problem avoidance or mitigation.

2. Riverine nutrient export to coastal seas

This project uses modeled river nutrient exports to the coast and inland (endorheic) drainages based on version 2 of the Global NEWS model ("Global NEWS 2"), described in detail in Mayorga et al. (2010). The geographically referenced basins cover the entire globe, excluding Antarctic and other permanently glaciated areas. Global NEWS 2 was developed as an advancement over the original Global NEWS models first published in 2005, particularly in support of a collaborative study of recent and possible future trends in nutrient inputs and exports (1970 – 2050) based on the Millennium Ecosystem Scenarios; the scenarios project is described in Seitzinger et al. (2010a). Nitrogen (N), phosphorus (P) and carbon (C) dissolved and particulate forms modeled by Global NEWS include DIN, DON, PN, DIP, DOP, PP, DOC and POC. The export of total suspended solids (TSS) is also modeled and included in this package.

Global NEWS 2 is implemented on the STN-30p version 6.01 (0.5 degree grid resolution) global river system, with the exclusion of permanently glaciated areas (grid cells); this pre-processing step eliminated most of Greenland and portions of some Arctic islands, leaving 6,081 basins, including 164 endorheic basins. See Mayorga et al. (2010) for more details and appropriate references.

2.1. Model run and files included in this package

There are 11 model runs included in this package. There are three near-contemporary conditions or historical runs for the year 1970 and 2000. Four scenarios are included in this package which are presented in Seitzinger et al. (2010a)based on the Millennium Ecosystem Scenarios assessment. The model run for 2030 and 2050 for each scenario is included in this package. The year-2000 reference model run used in the scenarios assessment is based on simulated climate and uncorrected modeled river discharge (Seitzinger et al., 2010a;Mayorga et al., 2010), which provides a consistent baseline for comparisons to outputs from scenarios of future conditions. The model output distributed here includes dissolved silica (DSi) exports based on the Global NEWS sub-model presented in Beusen et al. (2009) and implemented into the Global NEWS 2 modeling framework after Mayorga et al. (2010) was published; DSi results reflect only minor differences compared to those of Beusen et al. (2009).

This package includes the following components:

- This documentation file (*README_GlobalNEWS2ModeledExports.doc*)
- 11 Excel files (*<Code>NEWS.xls*) with the <Code> given in the table below corresponding to each model run. Each Excel file has four sheets, including "RIVER EXPORTS" (nutrient-form modeled exports as yields and loads), "BASINS" (general basin attributes and regions), "HYDROLOGY" (hydro-climate forcings), and "README" (documentation) briefly describing each data column. The naming scheme follows Mayorga et al. (2010); see supplementary Table A4 in that publication for an extensive listing of model variables.
- A polygon GIS shape file (*NEWS2basins.shp* and associated files) with every basin represented as a single multi-polygon (where some basins may have separate

polygon components that together make up a single basin). The only attribute included here is the STN-30p basin identifier as used throughout Global NEWS 2.

All basin-scale information and data may be linked across the tables and GIS shape file via the unique basin identifier ("basinid"). Consult relevant documentation and publications before using and interpreting Global NEWS 2 results found in this package. Please cite the appropriate Global NEWS publication in your work, including, as needed, original publications from 2005 that describe the development and validation of each nutrient sub-model in greater detail than Mayorga et al. (2010). As discussed in Global NEWS publications, results for small basins (less than ten 0.5^{o} grid cells) are unreliable as the watershed representations may have large errors; they should be used with caution and mainly as aggregated, regional summaries.

Table 2.1. Datafiles in the Global NEWS database

*.xls	Description
R00	"Realistic hydrology" for the reference year 2000. This run is only used for calibration and NOT for scenario analyses. DSi is not present in this run.
C70	Near-contemporary conditions or historical run for 1970
C00	Near-contemporary conditions or historical run for 2000
A30	For the year 2030 and with model assumptions of Adapting Mosaic (AM) for 2030, a world with a focus on regional and local socio-ecological management
A50	For the year 2050 and with model assumptions of Adapting Mosaic (AM) for 2050, a world with a focus on regional and local socio-ecological management
G30	For the year 2030 and with model assumptions of Global Orchestration (GO), a globalized world with an economic development focus and rapid economic growth
G50	For the year 2050 and with model assumptions of Global Orchestration (GO), a globalized world with an economic development focus and rapid economic growth
O30	For the year 2030 and with model assumptions of Order from Strength (OS), a regionalized world with a focus on security
O50	For the year 2050 and with model assumptions of Order from Strength (OS), a regionalized world with a focus on security

T30	For the year 2030 and with model assumptions of Technogarden (TG), a globalized world with a focus on environmental technology
T50	For the year 2050 and with model assumptions of Technogarden (TG), a globalized world with a focus on environmental technology

2.2. Availability and Contact Information

The Global NEWS 2 model and corresponding model inputs and outputs were developed by the Global NEWS group, an international work group of UNESCO's Intergovernmental Oceanographic Commission (IOC). Additional information may be found at the old Global NEWS site, http://www.marine.rutgers.edu/globalnews/, and the similar version at IOC:

http://www.ioc-unesco.org/icr/index.php?option=com_content&view=article&id=45&Itemid=100002

The Global NEWS 2 work described in these web sites is no longer being updated. The version described here is available from http://www.nutrientchallenge.org/filebrowser.

For questions and additional information, please contact Arthur Beusen (a.h.w.beusen@uu.nl), Utrecht University, The Netherlands.

2.3. Publications

Global NEWS data presented in this project are summarized in a series of papers (Yasin et al., 2010;Yan et al., 2010;van der Struijk and Kroeze, 2010;Thieu et al., 2010;Seitzinger et al., 2010b;Seitzinger et al., 2010a;Ludwig et al., 2010;Harrison et al., 2010a;Garnier et al., 2010;Fekete et al., 2010;Billen et al., 2010;Van Drecht et al., 2009;Bouwman et al., 2009;Beusen et al., 2009;Seitzinger et al., 2010c) in the Global NEWS 2 Special section of *Global Biogeochemical Cycles* "Past and Future Trends in Nutrient Export From Global Watersheds and Impacts on Water Quality and Eutrophication" (http://onlinelibrary.wiley.com/journal/10.1002/%28ISSN%291944-9224/specialsection/NUTRIENT1). The models of Global NEWS have been published in another special section "Global Nutrient Export From Watersheds"in 2005: (Van Drecht et al., 2005;Seitzinger et al., 2005;Harrison et al., 2005b;Harrison et al., 2005a;Dumont et al., 2005;Beusen et al., 2005).

Key publications

Mayorga, E., S.P. Seitzinger, J.A. Harrison, E. Dumont, A.H.W. Beusen, A.F. Bouwman, B.M. Fekete, C. Kroeze and G. Van Drecht. 2010. Global Nutrient Export from WaterSheds 2 (NEWS 2): Model development and implementation. *Environmental Modelling & Software* 25: 837-853, doi:10.1016/j.envsoft.2010.01.007

Seitzinger, S.P., E. Mayorga, A.F. Bouwman, C. Kroeze, A.H.W. Beusen, G. Billen, G. Van Drecht, E. Dumont, B.M. Fekete, J. Garnier and J.A. Harrison. 2010. Global river nutrient export: A scenario analysis of past and future trends. *Global Biogeochemical Cycles* 24: GB0A08, doi:10.1029/2009GB003587.

Beusen, A. H. W., A. F. Bouwman, H.H. Dürr, A.L.M. Dekkers and J. Hartmann. 2009. Global patterns of dissolved silica export to the coastal zone: Results from a spatially explicit global model. *Global Biogeochemical Cycles* 23: GB0A02, doi:10.1029/2008GB003281

Other publications in the 2010 Special Section on Global NEWS 2 of *Global Biogeochemical Cycles*

Billen, G., Beusen, A., Bouwman, L., Garnier, J., 2010. Anthropogenic nitrogen autotrophy and heterotrophy of the world's watersheds: Past, present, and future trends. Global Biogeochemical Cycles 24, GB0A11.

Bouwman, A.F., Beusen, A.H.W., Billen, G., 2009. Human alteration of the global nitrogen and phosphorus soil balances for the period 1970–2050. Global Biogeochemical Cycles 23, GB0A04.

Fekete, B.M., Wisser, D., Kroeze, C., Mayorga, E., Bouwman, L., Wollheim, W.M., Vörösmarty, C., 2010. Millennium Ecosystem Assessment scenario drivers (1970–2050): Climate and hydrological alterations. Global Biogeochemical Cycles 24, GB0A12.

Garnier, J., Beusen, A., Thieu, V., Billen, G., Bouwman, L., 2010. N:P:Si nutrient export ratios and ecological consequences in coastal seas evaluated by the ICEP approach. Global Biogeochemical Cycles 24, GB0A05.

Harrison, J.A., Bouwman, A.F., Mayorga, E., Seitzinger, S., 2010. Magnitudes and sources of dissolved inorganic phosphorus inputs to surface fresh waters and the coastal zone: A new global model. Global Biogeochemical Cycles 24, GB1003.

Ludwig, W., Bouwman, A.F., Dumont, E., Lespinas, F., 2010. Water and nutrient fluxes from major Mediterranean and Black Sea rivers: Past and future trends and their implications for the basin-scale budgets. Global Biogeochemical Cycles 24, GB0A13.

Seitzinger, S.P., Bouwman, A.F., Kroeze, C., 2010. Preface to special section on Past and Future Trends in Nutrient Export From Global Watersheds and Impacts on Water Quality and Eutrophication. Global Biogeochemical Cycles 24, GB0A01.

Thieu, V., Mayorga, E., Billen, G., Garnier, J., 2010. Subregional and downscaled global scenarios of nutrient transfer in river basins: Seine-Somme-Scheldt case study. Global Biogeochemical Cycles 24, GB0A10.

van der Struijk, L.F., Kroeze, C., 2010. Future trends in nutrient export to the coastal waters of South America: Implications for occurrence of eutrophication. Global Biogeochemical Cycles 24, GB0A09.

Van Drecht, G., Bouwman, A.F., Harrison, J., Knoop, J.M., 2009. Global nitrogen and phosphate in urban wastewater for the period 1970 to 2050. Global Biogeochemical Cycles 23, GB0A03.

Yan, W., Mayorga, E., Li, X., Seitzinger, S.P., Bouwman, A.F., 2010. Increasing anthropogenic nitrogen inputs and riverine DIN exports from the Changjiang River basin under changing human pressures. Global Biogeochemical Cycles 24, GB0A06.

Yasin, J.A., Kroeze, C., Mayorga, E., 2010. Nutrients export by rivers to the coastal waters of Africa: Past and future trends. Global Biogeochemical Cycles 24, GB0A07.

Global NEWS publications in the 2005 Special Section on Global NEWS of *Global Biogeochemical Cycles*

Beusen, A.H.W., Dekkers, A.L.M., Bouwman, A.F., Ludwig, W., Harrison, J., 2005. Estimation of global river transport of sediments and associated particulate C, N, and P. Global Biogeochemical Cycles 19, GB4S05.

Dumont, E., Harrison, J.A., Kroeze, C., Bakker, E.J., Seitzinger, S.P., 2005. Global distribution and sources of dissolved inorganic nitrogen export to the coastal zone: Results from a spatially explicit, global model. Global Biogeochemical Cycles 19, GB4S02.

Harrison, J.A., Caraco, N., Seitzinger, S.P., 2005a. Global patterns and sources of dissolved organic matter export to the coastal zone: Results from a spatially explicit, global model. Global Biogeochemical Cycles 19, GB4S04.

Harrison, J.A., Seitzinger, S.P., Bouwman, A.F., Caraco, N.F., Beusen, A.H.W., Vörösmarty, C.J., 2005b. Dissolved inorganic phosphorus export to the coastal zone: Results from a spatially explicit, global model. Global Biogeochemical Cycles 19, GB4S03.

Seitzinger, S.P., Harrison, J.A., Dumont, E., Beusen, A.H.W., Bouwman, A.F., 2005. Sources and delivery of carbon, nitrogen, and phosphorus to the coastal zone: An overview of Global Nutrient Export from Watersheds (NEWS) models and their application. Global Biogeochemical Cycles 19, GB4S01.

Van Drecht, G., Bouwman, A.F., Boyer, E.W., Green, P., Siebert, S., 2005. A comparison of global spatial distributions of nitrogen inputs for nonpoint sources and effects on river nitrogen export. Global Biogeochemical Cycles 19, GB4S06.

3. Nutrient release from aquaculture

3.1. Description of the data

A model was developed by Bouwman et al. (2011) to estimate nitrogen (N) and phosphorus (P) country budgets for aquaculture production of individual species within crustaceans, bivalves, gastropods and seaweed, using country production data for the 1970-2010 period from the Food and Agriculture Organization, and scenarios based on the Millennium Assessment for 2010-2050.

A similar global model was developed by Bouwman et al. (2013a) to calculate feed and nutrient budgets for freshwater and marine omnivorous and carnivorous aquaculture finfish production. The model uses national production data for the period 1970-2010 and the Millennium Ecosystem Assessment scenarios for production and management for 2010-2050.

The data from the latter study was used in a paper (Bouwman et al., 2013b) that compares the magnitude and changes of nutrient release in different countries (China, Chile, Mexico). Nutrients from freshwater, brackishwater marine aquaculture (mariculture) are allocated in specific parts of Chile and Mexico.

This chapter describes the spatial allocation of nutrient release at 0.5 by 0.5 degree resolution (consistent with Global NEWS as described in Chapter 2) by aquaculture for freshwater aquaculture and mariculture for all countries of the world.

3.2. Allocation of nutrient release from freshwater aquaculture

General

The production of aquaculture is now given by the Food and Agriculture Organization of the United Nations (FAO) FishStat database (FAO, 2013) for each country and for each species, type of environment (marine, brackish, freshwater), and sea. Although the Food and Agriculture Organization of the United Nations (FAO) has a wealth of information available on aquaculture production by farm or production system within a range of countries for different species and environments (see http://www.fao.org/fishery/collection/naso-maps/en and http://www.fao.org/fishery/naso-maps/fact-sheets/en/), it is still difficult to obtain global spatially explicit data on where aquaculture production is located.

For distributing the aquaculture production (P) of a country spatially (here 0.5 by 0.5 degree grid cells), we developed an allocation procedure based on a weighting factor map. To construct the weighting map, we made use of expert judgment (see next

paragraph). The weighting factors *W* range from 0 (no chance to find any *P*), to an arbitrary maximum value (very likely to find *P*), so *W* and *P* must be positively correlated.

The weighing factor map construction

The weighing factor map is built as a combination of three factors that influence the location of the aquaculture production:

- Population density
- Presence of water bodies
- Temperature.
-

Population density

Population density was used as a proxy for aquaculture production, assuming that most fish production takes place close to populated areas. Two major assumptions are: (i) when there are no people living in a grid cell, a low probability of aquaculture production is assumed (q = 0.01); (ii) for high population densities (above x_{end} =10000 inhabitants/km^2), the probability of aquaculture production is also low (q = 0.01). The optimum population density (x_{opt}) is around 1000 inhabitants per square kilometer. We use the following approach based on a two parabolic functions with the equation:

$$W_{population} = ax^2 + bx + c$$

Where x = population density, and $W_{population}$ =probability of aquaculture production based on population. The values for a, b and c depend on the population density:

For x < 0 and x > 10000: $y = q$

For the left part of the function ($x < x_{top}$):
$a = (q\text{-}1)/x_{top}^2$
$b = -2a^*x_{top}$
$c = q$

For $x_{top} < x < 10000$:
$a = (q\text{-}1)/(x_{top}\text{-}10000)^2$
$b = -2a^*x_{top}$
$c = 1 + ax_{top}^2$

Presence of water bodies

The Global Lakes and Wetlands Database (GLWD) (Lehner and Döll, 2004) has twelve different types of water bodies (see Table 3.1). For each type of water body, we estimated the probability that freshwater aquaculture can occur. The probabilities $W_{waterbody}$ for each type of water body are in the table below.

Temperature

Aquaculture is not possible in regions with low temperatures. We therefore use the criterion that there is no aquaculture production in cold regions. Since global water temperature data are not available, we use mean annual air temperature as a proxy, and the limit is taken as 0°C, hence $W_{\text{temperature}} = 0$ for annual temperature <0°C. This is slightly lower than the limit for air temperature, because water temperatures normally lag behind those of air.

Overall weighing factor

The overall probability of finding aquaculture in a grid cell is calculated as follows:

$$W_{\text{overall}} = W_{\text{population}} W_{\text{waterbody}} W_{\text{temperature}}$$

We use the population density and water temperature for the year 2000 and use these weighing factors for all years. So weighing factors are independent in time.

Table 3.1. Probability of occurrence of freshwater aquaculture for water bodies distinguished in the Global Lakes and Wetlands Database (GLWD) (Lehner and Döll, 2004)

#	GLWD class	$W_{\text{waterbody}}$
1	No data, or no waterbody.	0.1
2	Lake	1.0
3	Reservoir	1.0
4	River	1.0
5	Freshwater Marsh, Floodplain	0.5
6	Swamp Forest, Flooded Forest	0
7	Coastal Wetland (incl. Mangrove, Estuary, Delta, Lagoon)	0
8	Pan, Brackish/Saline Wetland	0
9	Bog, Fen, Mire (Peatland)	0
10	Intermittent Wetland/Lake	0.5
11	50-100% Wetland	1.0
12	25-50% Wetland	1.0
13	Wetland Complex (0-25% Wetland)	0.5

Allocation

Allocation for finfish and shellfish is calculated separately. The allocation takes place in two steps: (i) all grid cells with $W_{overall}$ < 10% of the maximum value in that country. This excludes the grid cells with lowest probability. (ii) aquaculture production is allocated to the remaining grid cells based on the ratio of the probability of the grid cell and the sum of probabilities of all grid cells within that country. (ii) Subsequently, all grid cells with a production <1000 kg fresh fish are excluded. The weighing factor for these cells are set to 0, and the allocation procedure is repeated. Where the country production is smaller than this minimum, one grid cell is allocated. Allocation by weighing is done by the following equations:

$$P(i) = [\frac{W(i)}{SW(j)}]$$

$$SP(j) \leq Pmax(i)$$

Where *P*(i) = allocation variable in cell i (unit), *W*(i) = weighing variable in cell i (any unit), *SW*(j)= sum of weights *W*(i) of region j (any unit), *SP*(j)= sum of all values of allocated variable *P*(i) of region j (unit), and *P*max(i) = maximum value of *P*(i) in cell i (unit).

In the process of allocating the production *P* to grid cells i of country i, temporally *P*(i) may exceed *P*max(i). In that case, we have a residual Pres in grid cell i. The sum of all residual *P*'s of region j, *SP*res(j) must be allocated in the next round in cells, where we still have allocation space left, i.e. *P*max-*P* > 0. The allocation process is completed when all the *SP* is allocated. Grid cells that remain after these two steps, are assigned N and P emissions to surface water from freshwater aquaculture on basis of $W_{overall}$. The resulting spatial distributions for N and P release from freshwater aquaculture are presented in Figures 3.1a and 3.2a.

3.2 Allocation of nutrient release from mariculture

Mariculture production consists of brackish water aquaculture and marine aquaculture. These two types have different allocation procedures. Nutrients released by brackish water aquaculture production are allocated to coastal land grid cells (bordering the sea) with human population density and temperature as a weighing factor, following the procedures discussed above for freshwater aquaculture.

Nutrient releases from mariculture are allocated to coastal grid cells (sea cells bordering coastal land cells) on the basis of length of the coastline (obtained from ARCGIS), as a proxy for the presence of bays or other coastal waters partly sheltered from the influence of the open sea, i.e. places where aquaculture production could occur.

In addition to length of the coastline, aquaculture production is allocated preferentially in specific coastal types, taken from the work of Dürr et al. (2011). Tidal systems (estuaries, rias and embayments), Fjords and Fjaerds are assigned a weighing factor of 10, small deltas are assigned a weighing factor of 5, and all other coastal types a weighing factor of 1 (endorheic or

glaciated, lagoons, large rivers bypassing the near-shore coastal zone, large rivers with tidal deltas, karst and arrheic coasts). Finally, temperature was used as a weighing factor following the procedure described above for freshwater aquaculture allocation.

During the allocation, grid cells that are assigned fresh-weight production of <1000 kg yr^{-1} are excluded; the weighing factor for these cells are set to 0, and the allocation procedure is repeated. The resulting spatial distributions for N and P release from brackish water aquaculture are shown in Figures 3.1b and 3.2b respectively, and for mariculture in 3.1c and 3.2c, respectively. The data for mariculture were used in Chapter 4 to compute the N sources by COSCAT region.

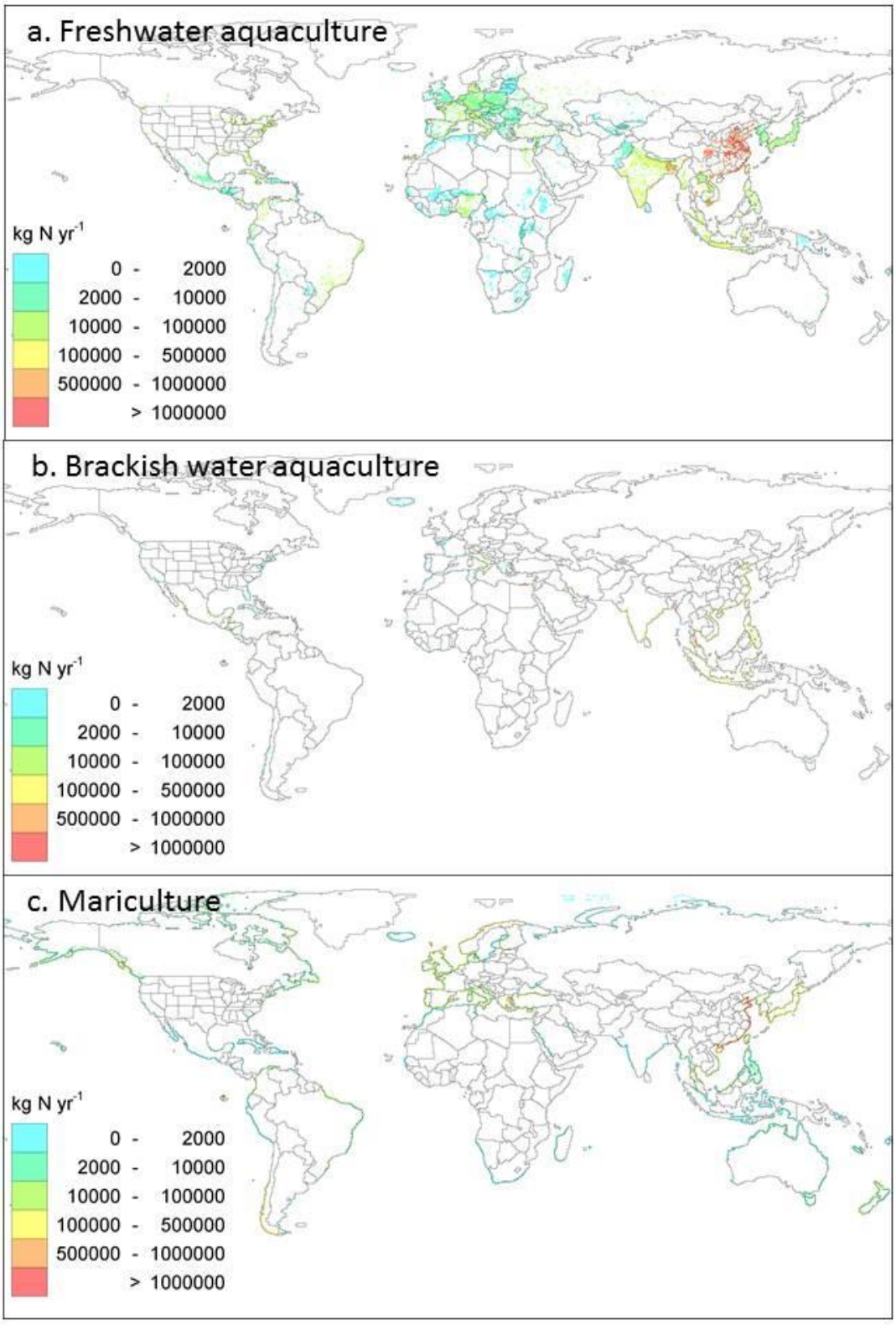

Figure 3.1. N release from (a) freshwater , (b) brackish water, and (c) and marine aquaculture.

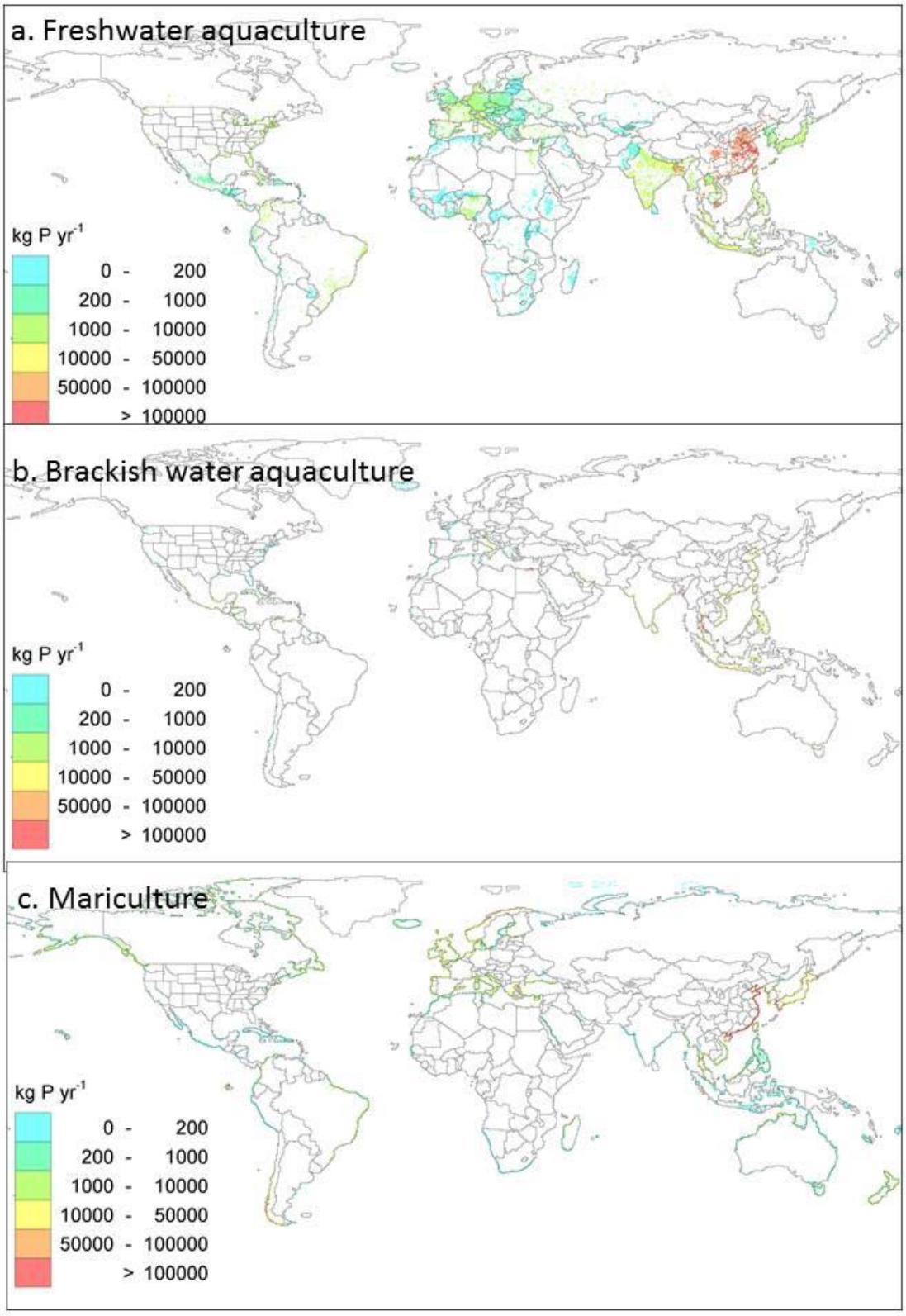

Figure 3.2. P release from (a) freshwater, (b) brackish water, and (c) and marine aquaculture.

4. Coastal conditions and coastal effects

This chapter describes the collection and development of data needed to describe the physical and environmental conditions in coastal marine ecosystems worldwide.

4.1. Spatially explicit global database of coastal characteristics

A database has been developed that includes information about nutrient loading to the global coastal ocean and associated effects of nutrient loading. Although information about several inputs is available at finer spatial and temporal scales, the level of coastal segments with their corresponding river catchments (COSCAT) resolution (Laruelle et al., 2013) was selected, because this was the finest resolution at which we could attain all necessary coastal parameters. Specific parameters included in the database are listed in Table 4.1. This database is the most comprehensive and up-to-date collection of coastal characteristics of which we are aware.

Many of these inputs were available from established sources. When this was the case, we simply compiled and spatially averaged data by COSCAT region. Such inputs included river basins, receiving COSCAT for each of the Global NEWS basins, average salinity (g/kg), average temperature (^{o} C), mean depth (m), average tide amplitude, typology for receiving waterbody, average surface NO_3 concentration, average surface PO_4 concentration, river N, P, Si, and C loading, and N from submarine groundwater.

4.2. Datasets developed for this project

When estimates of coastal characteristics or nutrient fluxes were not available, we had to develop them. Our methods for developing estimates of these inputs and characteristics are described below.

Receiving COSCAT

It was necessary to spatially associate each Global NEWS river basin with its receiving COSCAT (Laruelle et al., 2013). This was achieved by performing a spatial join within ArcMap 10.0.

Freshwater flushing time

Freshwater flushing time (T_{fw}), often used as a proxy for freshwater residence time, was calculated as

$$T_{\mathrm{fw}} = \frac{V}{Q}$$

where *V* is the volume of the receiving COSCAT and *Q* is the total river discharge estimated to enter the receiving water body. Volume (*V*) of coastal receiving waterbody was calculated as the product of horizontal surface area and mean depth (Table 4.1).

N Upwelling

We were unable to identify an existing estimate of N upwelling in coastal regions, so we developed one. We estimated N upwelling (N_{up}) according to:

$$N_{\text{up}} = [N]\, W\, A_{\text{h}}$$

Where N is nitrate concentration just below the mixed layer depth (mg NO_3-N l^{-1}), W is the vertical velocity at the mixed layer depth, and A_h is the horizontal cross-sectional area of each half-degree cell within the water body being analyzed. Upwelling in individual half-degree cells was averaged in COSCAT analysis in order to attain a mean upwelling input. Values of N were taken from the World Ocean Atlas. *W* was calculated as an average of vertical velocities reported in the ODA GFDL project. A_h was calculated as in Harrison et al. (2010).

N Onwelling

As with upwelling, we were unable to identify an existing spatially-explicit estimate of coastal N onwelling, so we developed one. We estimated coastal N onwelling (N_{on}) as follows:

$$N_{\text{on}} = \sum_{0}^{MLD} [N]\ U\ A_{\text{v}} + [N]\ V\, A_{\text{v}}$$

where N is average reported NO_3 concentration at a given depth, *MLD* is the depth of the mixed layer,

U is velocity in the west-east direction (with positive U values indicating eastward flows), *V* is velocity in the south-north direction (with positive V values indicating northward flows),

A_v is the surface area of the cross-section of each cell perpendicular to the direction of water flux (i.e. thickness of layer times length of grid cell side).

Table 4.1. Coastal conditions, nutrient delivery and impacts database.

Parameter	Source	Resolution	Coverage
	Coastal Characteristics		
COSCAT, including ocean, continent, and surface area	Dürr et al. (2011), Laruelle et al. (2013)	COSCAT	Global
River basins	Fekete et al. (2002)	0.5 degree	Global
Receiving COSCAT for each of the Global NEWS basins	Developed for this project [a]	COSCAT	Global
Average salinity (g/kg)	World Ocean Atlas 2009 (NOAA, 2009)	COSCAT	Global
Average temperature (^{o} C)	World Ocean Atlas 2009 (NOAA, 2009)	COSCAT	Global
Mean depth (m)	updated ETOPO5 (Egbert and Erofeeva, 2002)	COSCAT	Global
Mixed layer depth (m)	World Ocean Atlas 2009 (NOAA, 2009)	COSCAT	Global
Exchange coefficient between surface & deep waters (yr^{-1})	Developed for this project (described in text)	COSCAT	Global
Buoyancy frequency (s^{-2})	Calculated from salinity and temperature (see table entries above)	COSCAT	Global
Average tide amplitude	Egbert and Erofeeva (2002)	COSCAT	Global
Typology for receiving waterbody	Dürr et al. (2011), Laruelle et al. (2013)		Global
Average surface NO_3 concentration	World Ocean Atlas 2009 (NOAA, 2009)	COSCAT	Global
Average surface PO_4 concentration	World Ocean Atlas 2009 (NOAA, 2009)		Global
River N, P, Si, and C loading (Global NEWS, Chapter 2)	Mayorga et al. (2010), Seitzinger et al. (2010c)	COSCAT	Global
N and P release from aquaculture	Developed for this project [a]	0.5 degree	Global
N from submarine groundwater	Beusen et al. (2013)	COSCAT	Global
N Onwelling	Developed for this project [a]	COSCAT	Global
N Upwelling	Developed for this project [a]	COSCAT	Global
Richardson number	Developed for this project [a]	COSCAT	Global
Freshwater flushing time	Developed for this project [a]	COSCAT	Global
N Deposition (kg N km^{-2} yr^{-1})	Lamarque et al. (2013)	COSCAT	Global
Single greatest N source	Developed for this project [a]	COSCAT	Global
	Coastal Impacts		
Occurences of hypoxia	WRI 2015	COSCAT	Global
Occurences of HABs	HAEDAT, SCOR 132, SOA (2014)	COSCAT	Global
Average annual Chl *a* concentration	Sea WIFS and MODIS, http://oceancolor.gsfc.nasa.gov/	COSCAT	Global
Average annual primary production	Behrenfeld et al. (2005)	COSCAT	Global

[a] See text.

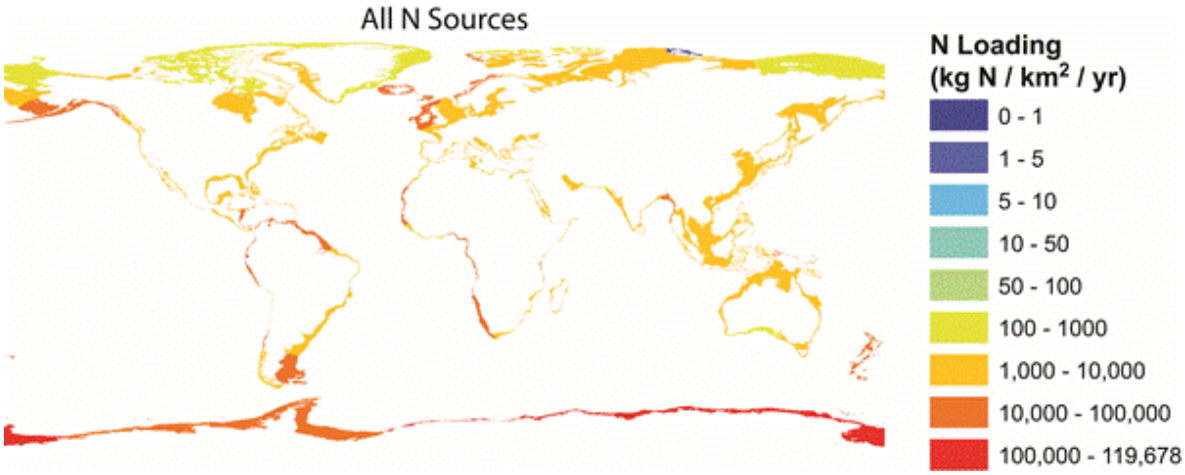

Figure 4.1. Total N delivered to coastal zones globally (all marine and terrestrial sources), resolved at the scale of COSCATs. Sources are listed in Table 4.1.

Mass of N transfer was calculated for each depth range and summed to calculate total mass transferred from non-coastal half-degree cells to coastal 0.5 degree grid cells within the mixed layer. N transfer to all half-degree cells at the seaward edge of each COSCAT was then summed to estimate a total net N onwelling value. Depth intervals for which N transfer masses were calculated were as follows: 0-10m, 10-20m, 20-30m, 30-50m, 50-75m, 75-100m, 100-125m, 125-150m, and 150-200m.

Richardson number

Richardson number (R_i), an indicator of water column stratification and stability, was calculated as follows:

$$R_i = \left(\frac{\rho' - \rho}{\bar{\rho}}\right)\left(\frac{h}{TA}\right)^2$$

Where ρ' represents water density at the bed, ρ represents water density at the surface, $\bar{\rho}$ is average water density, h is water depth, and TA is tidal amplitude. High R_i values indicate well-stratified, stable conditions, whereas low R_i values (e.g. <0.25) indicate weakly stratified or well-mixed systems.

Buoyancy Frequency

Buoyancy frequency, N^2, provides a measure of water column stratification. As we are interested in exchange between surface and deep waters, we consider buoyancy

frequency at the pycnocline, which delineates these two regions. At this point, the buoyancy frequency achieves its maximum value defined as

$$N^2_{\max} = \max\left(-\frac{g}{\rho}\frac{\partial \rho}{\partial z}\right)$$

4.3. Results of source analysis

Figure 4.1 shows the total N input by COSCAT region. Figures 4.2 and 4.3 show land-based N sources and the marine-derived N sources, respectively. Understanding the relative contribution to coastal N loading from various sources is critical if we are to attempt to manage coastal N loading. For example, human activities may be modified to reduce N loading from rivers and the atmosphere, but management of onwelling and upwelling sources is not currently possible. To our knowledge this is the first analysis that explicitly compares different N sources to the coastal zone. This first-cut analysis indicates that river N was the greatest N source to 47% of COSCATS, while N fixation, onwelling, upwelling, and N deposition were the largest sources in 20%, 19%, 13%, and 1% of COSCATs, respectively. There were no COSCATs in which groundwater N inputs dominated.

Somewhat surprisingly, some of the highest rates of coastal N loading were estimated to occur in COSCATs with very little human activity, for example around Antarctica and along the northern and southern coasts of Alaska (Figure 4.1). This was due largely due to high onwelling sources of N and P in these regions (Figure 4.3). Future efforts will focus on quantifying the anthropogenic portion of river and atmospheric deposition to coastal systems.

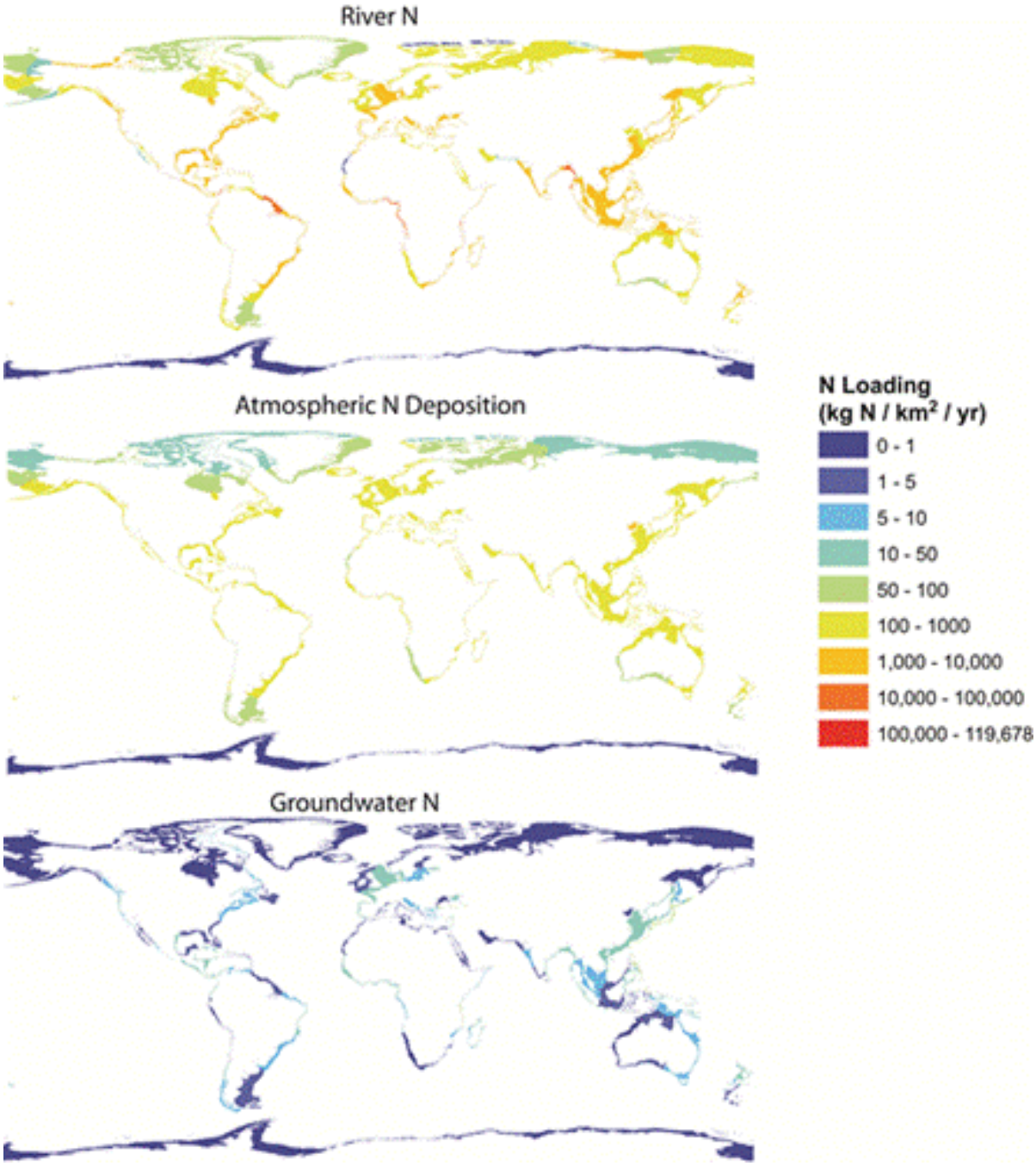

Figure 4.2. Land-based sources of N to coastal zones globally, resolved at the scale of COSCATs. Sources are listed in Table 4.1.

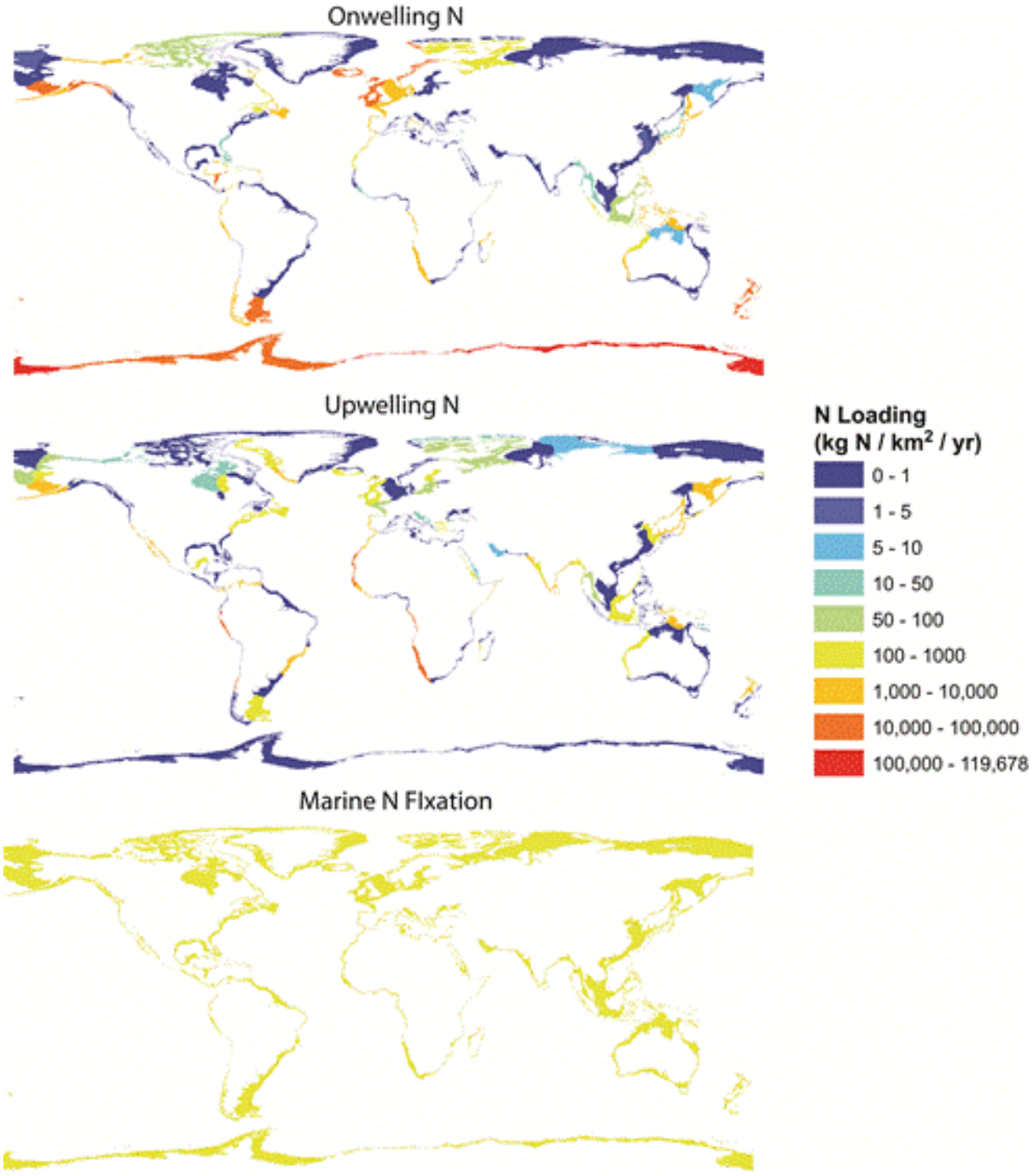

Figure 4.3. Marine-derived sources of N to coastal zones globally, resolved at the scale of COSCATs. Sources are listed in Table 4.1.

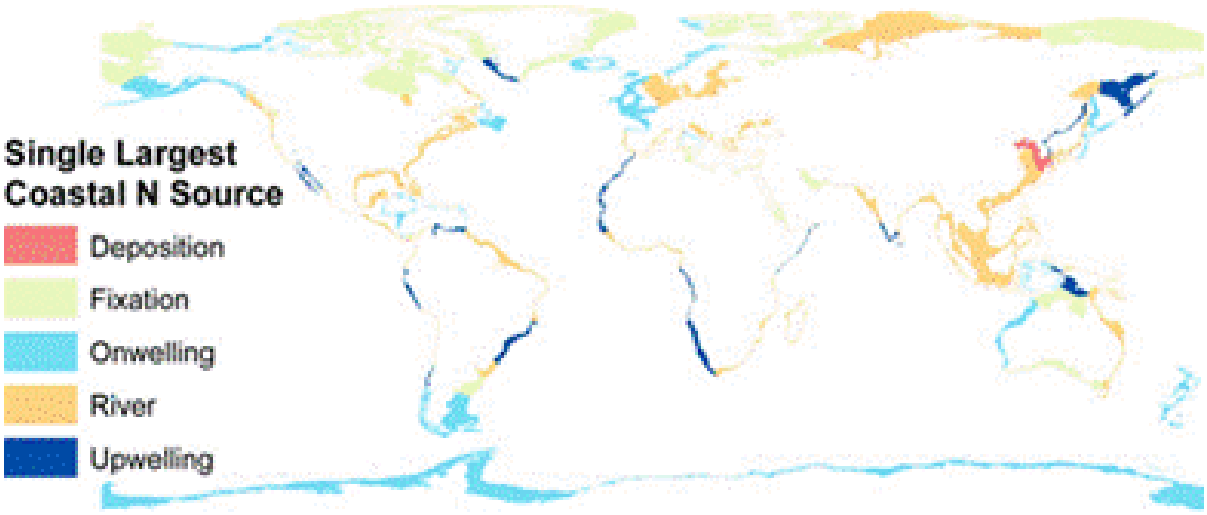

Figure 4.4. COSCATS globally, color coded according to the single largest N source in each COSCAT.

5. Observed impacts

5.1. Occurrences of hypoxia

We attained records of 479 hypoxic event locations, decade of occurrence, and hypoxia type from the World Resources Institute (WRI) (http://www.wri.org/resources/data-sets/eutrophication-hypoxia-map-data-set). In this dataset, hypoxic regions are categorized by type, including persistent, periodic, and seasonal categories (Figure 5.1). Many, though not all, of these systems were included in Diaz and Rosenburg (2009). These data were downloaded, processed, and individual occurrences of hypoxia were linked to COSCAT regions.

Within this dataset there is a striking increase in occurrences and cumulative surface area of hypoxic events over the past several decades, with improvement in conditions only occurring in a small fraction of coastal systems. Spatially, the highest concentrations of hypoxic events are reported to occur along the east and gulf coasts of the US, in the Baltic region, and off the coast of Japan. There are also regions of hypoxia in the northwest US, along the coasts of Argentina, and on the southwest coast of Australia. There is a surprising absence of reported hypoxia in much of the tropics. This may be due to underreporting resulting from a lack of consistent monitoring efforts in these regions, highlighting a need for models capable of predicting hypoxia in regions with little data.

We also collected information about water column O_2 concentrations from the World Ocean Atlas (WOA) and evaluated the spatial correspondence between low O_2 bottom waters in the WOA dataset and the reported instances of hypoxia in the WRI dataset. Perhaps due to differences in spatial and temporal scale, and sometimes lack of spatial overlap, between the two datasets (e.g. some hypoxic events were reported for estuarine or lagoon systems in regions not covered by WOA data), regions of reported hypoxia were not always regions with low reported bottom water O_2 concentrations in the global [O_2] dataset. Reconciling reported O_2 concentrations with reported hypoxic events remains a challenge.

5.2. Occurrences of algal blooms

Data on observed occurrences of harmful algal blooms was collected from three sources, i.e. the IOC HAEDAT database, the SCOR Workgroup 132 on harmful algal blooms, and Chinese data from State Oceanic Administration. A number of illnesses, major vectors and symptoms related to harmful algal blooms is listed in Table 5.1.

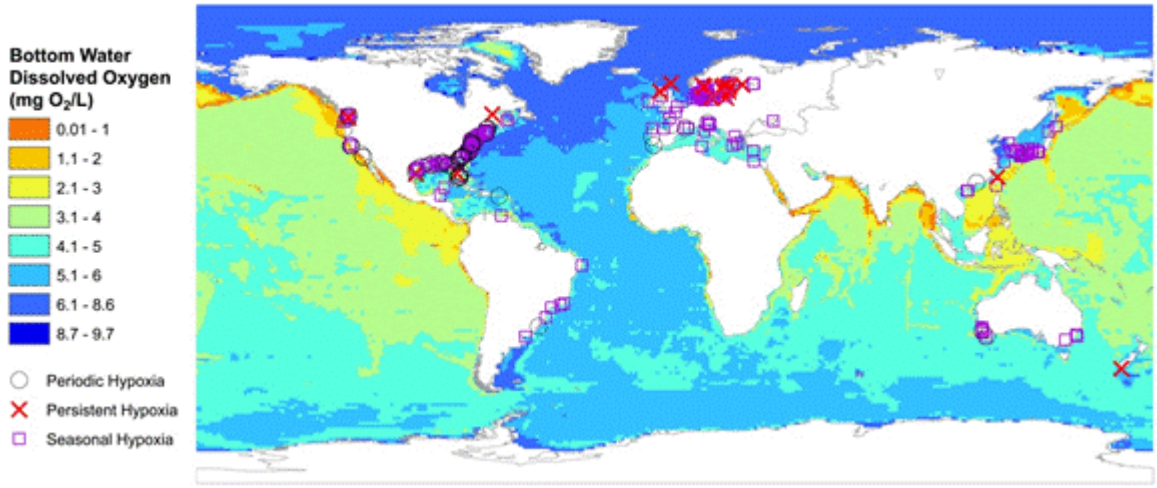

Figure 5.1. Bottom water O_2 concentrations globally and locations of observed hypoxia (Source: WRI, http://www.wri.org/resources/data-sets/eutrophication-hypoxia-map-data-set).

Table 5.1. Illnesses, major vectors and symptoms of HABs.

Illness	Major vector	Symptoms
Amnesic shellfish poisoning (ASP)	Domoic acid from *Pseudo-nitschia* sp. in shellfish	Short-term memory loss, vomiting, cramps
Diarrhetic shellfish poisoning (DSP)	Okadaic acid from *Dinophysis* sp. in shellfish	Diarrhea, vomiting, cramps
Neurotoxic shellfish poisoning (NSP)	Brevetoxin from *Karenia* sp. In shellfish, aerosolized toxins	Nausea, diarrhea, respiratory distress
Paralytic shellfish poisoning (PSP)	Saxitoxin from *Alexandrium* and other sp. in shellfish	Numbness around lips and mouth, respiratory paralysis, death
Cyanobacterial toxins effects (CTE)	Microcystins and other toxins from cyanobacteria in water	Skin irritation, respiratory irritation, tumor promotion

Observed harmful blooms were collected from the HAEDAT database hosted by Intergovernmental Oceanographic Committee (IOC) (http://haedat.iode.org/index.php). HAEDAT is a meta database containing records of harmful algal events. HAEDAT contains records from the ICES area (North Atlantic) since 1985, and from the PICES area (North Pacific) since 2000 (Figures 5.2 and 5.3). IOC Regional networks in South America and North Africa are preparing to contribute.

HAEDAT is part of the Harmful Algal Information System (HAIS) and will, when fully established, consist of access to information on harmful algal events, harmful algae monitoring and management systems worldwide, current use of taxonomic names of harmful algae, and information on biogeography of harmful algal species. Supplementary components are an expert directory and a bibliography.

The HAEDAT database was downloaded and converted to ASCII format and each observed HAB (by type) was assigned to the corresponding COSCAT regions. Subsequently, the correlation between the average number of events (number of events divided by the number of years with observations) and the factors described in Chapter 4 (Table 4.1) was computed by event syndrome. These include ASP = Amnesic shellfish poisoning; ATE = Aerosolized toxins effects; AZP, Azaspiracid shellfish poisoning; CTE, Cyanobacterial toxins effects; DSP, Diarrhetic shellfish poisoning; NSP, Neurotoxic shellfish poisoning; PSP, Paralytic shellfish poisoning; Other, any other bloom type; "0", type not recorded. Results are presented in Table 5.2.

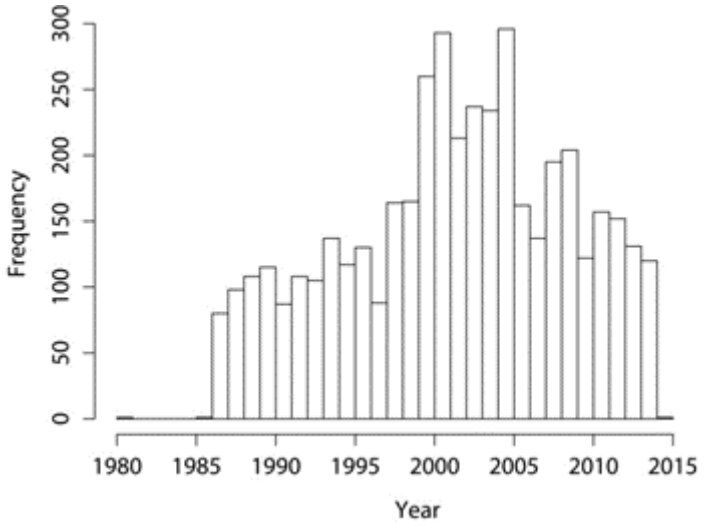

Figure 5.2. Number of reported harmful algae blooms globally on an annual basis between 1980 and 2015 (Source: HAEDAT database, (http://haedat.iode.org/index.php)).

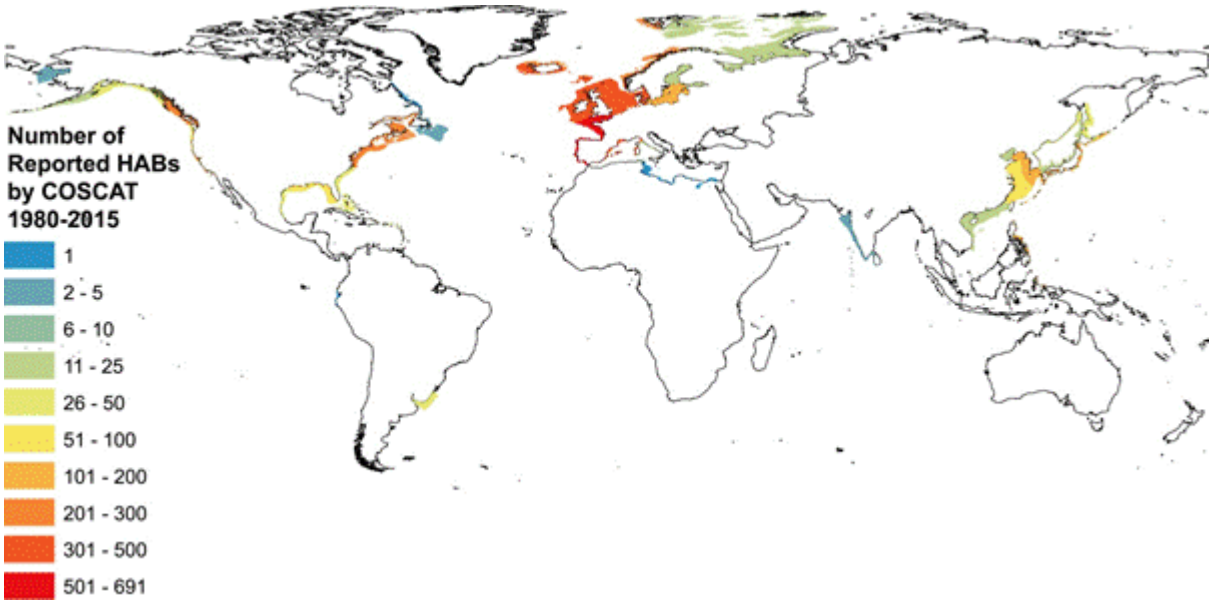

Figure 5.3. The number of reported harmful algae blooms from HAEDAT database between 1980 and 2015 by COSCAT coastal segment.

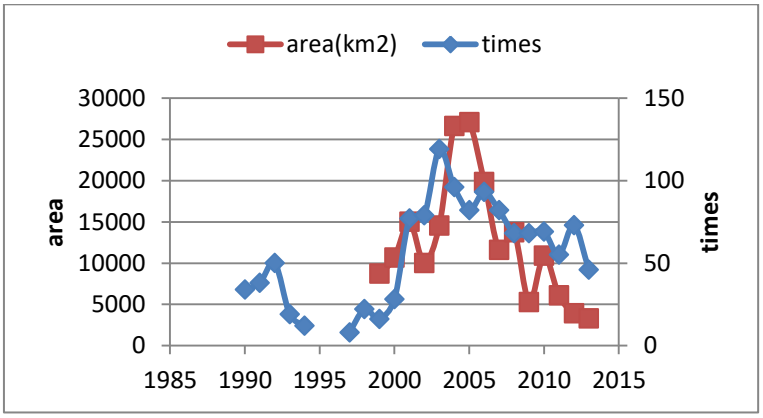

Figure 5.4. Area and frequency of observed algal blooms in Chinese coastal waters. Source: SOA (2014).

Table 5.2 provides a first summary of the HAEDAT database. The correlation is expressed as the correlation coefficient *r*, and the sign indicates a positive or negative effect of the parameter on the average number of observed occurrences. The salmon boxes indicate positive *r* values > 0.25, and green boxes negative values <-0.25. It is clear that none of the parameters clearly explains why blooms occur. However, the data show some first broad factors that have a general influence for a range of HAB species.

The first column in Table 5.2 for the total of all observed blooms indicates that a number of parameters have a large influence, including the mean depth and mixed layer depth (+, positive influence), primary production (-), benthic and total oxygen demand (-), buoyancy (+), N deposition and submarine groundwater discharge (+). The primary production shows the same negative correlation with different algae (ASP, DSP), and positive for cyanobacteria. Similarly, the depth of the water columns has a large and positive influence on occurrences of DSP and PSP. Mixed layer depth is an important factor for nearly all HABs except cyanobacteria.

Table 5.2. Analysis of the correlation (r) between parameters listed in Chapter 4 and observations in average number of occurrences in years with reported HABs for different bloom types[a].

Parameter	Total	ASP	0	DSP	AZP	OTHEF	ATE	NSP	PSP	CTE
Volume_(1000_km3)	0.20	0.09	0.17	0.15	0.60	0.01	-0.09	-0.08	0.06	-0.13
Surface_area_(1000_km2)	0.15	0.08	0.19	0.03	0.55	0.05	-0.11	0.00	-0.04	-0.08
Mean_depth_(m)	0.33	0.18	0.06	0.47	0.19	-0.06	0.01	-0.16	0.41	-0.22
Richardson_number_(mean)	0.02	0.04	0.13	-0.02	-0.12	-0.04	0.79	-0.08	-0.11	0.17
Mean_surface_salinity_(ppt)	0.14	0.15	0.02	0.14	0.11	-0.07	0.13	0.00	0.12	-0.75
Mean_surface_temperature_(C)	-0.04	-0.27	0.14	-0.23	-0.32	-0.20	0.08	-0.09	-0.10	-0.21
Water_input_(km3_y)	0.10	0.26	0.12	0.01	0.04	0.51	-0.10	0.57	-0.02	-0.05
Residence_time_(yr):_volume_(V)_over_flow_(Q)	-0.13	-0.15	-0.11	-0.10	-0.01	-0.11	-0.04	-0.08	-0.11	-0.09
Hydraulic_load_(m_per_y)	-0.08	0.19	-0.11	0.01	-0.16	0.27	-0.04	0.31	-0.02	0.05
Hydraulic_load_as_fraction_of_depth_(per_yr)	-0.17	0.03	-0.15	-0.12	-0.18	0.24	-0.06	0.32	-0.14	0.12
Mean_primary_production_(g_C_per_m2_per_d)	-0.25	-0.28	-0.05	-0.30	-0.20	-0.04	-0.14	0.00	-0.25	0.34
Max_bottom_water_O2_(ml_per_l)	0.06	0.11	-0.03	0.17	0.29	0.20	-0.09	0.12	-0.05	0.33
Min_bottom_water_O2_(ml_per_l)	-0.09	0.05	-0.09	0.03	0.32	0.03	0.05	-0.02	-0.22	0.37
Mean_bottom_water_O2_(ml_per_l)	-0.01	0.07	0.01	0.04	0.30	0.18	-0.03	0.11	-0.22	0.41
Sum_of_onwelling_water_flux_(km3_per_y)	0.04	-0.09	0.00	0.04	0.61	0.03	-0.02	0.03	0.12	-0.04
Sum_of_absolute_onwelling_water_flux_(km3_per_y)	0.09	-0.18	0.17	-0.06	0.47	-0.02	-0.03	-0.03	0.22	-0.07
Onwelling_water_flux_(km3_per_y)	0.12	-0.13	0.18	-0.03	0.48	-0.01	-0.02	-0.01	0.25	-0.11
Marine_residence_time_(y)	-0.01	0.14	0.06	0.04	-0.11	-0.08	-0.07	-0.10	0.02	-0.08
River_residence_time/marine_residence_time	-0.16	-0.24	-0.09	-0.14	0.03	-0.12	-0.03	-0.08	-0.12	-0.09
Mixed_layer_depth_(m)_from_gfdl_model	0.33	0.32	0.13	0.40	0.78	0.01	0.09	-0.11	0.18	-0.19
Volume_of_mixed_layer_(km3)	0.22	0.21	0.12	0.24	0.84	0.02	-0.08	-0.06	0.01	-0.12
Mixed_layer/mean_depth_(unitless)	-0.10	-0.08	-0.02	-0.15	0.29	-0.03	0.02	0.04	-0.18	-0.08
Seasonal_Hypoxia_Count	0.22	0.15	0.25	-0.03	0.03	0.03	-0.04	0.02	0.15	0.10
Persistent_Hypoxia_Count	0.12	0.16	0.08	0.06	0.19	0.19	-0.07	0.17	-0.05	0.19
Persistent_+_seasonal	0.23	0.17	0.25	-0.02	0.05	0.05	-0.04	0.04	0.14	0.12
Benthic_oxygen_demand_(mol_per_m2_per_year)	-0.26	-0.28	-0.05	-0.31	-0.20	-0.04	-0.13	0.00	-0.26	0.34
Water_column_oxygen_demand_(mol_per_m2_per_year)	-0.09	-0.20	0.04	-0.13	-0.15	-0.05	-0.17	-0.08	-0.04	0.32
Total_oxygen_demand_(mol_per_m3_per_year)	-0.29	-0.30	-0.11	-0.31	-0.18	-0.06	-0.10	0.01	-0.29	0.21
Mean_max_buoyancy_frequency_(per_s2)	0.33	0.38	0.08	0.48	0.17	0.05	0.17	-0.07	0.39	-0.18
Median_oxygen	0.00	0.15	0.01	0.05	0.41	0.08	0.02	0.04	-0.21	0.17
Per_area_DIN_(kg_N_per_km2_per_yr)	0.29	0.31	0.22	0.23	-0.22	0.42	0.07	0.45	0.21	-0.13
Per_area_DON_(kg_N_per_km2_per_yr)	0.04	0.32	-0.01	0.12	-0.18	0.37	-0.02	0.41	0.09	-0.08
Per_area_particulate_N_(kg_N_per_km2_per_y)	0.07	0.08	0.09	0.04	-0.19	-0.04	0.04	0.00	0.25	-0.15
Per_area_total_N_(kg_N_per_km2_per_y)	0.18	0.29	0.14	0.17	-0.23	0.33	0.04	0.37	0.21	-0.13
Per_area_DIP_(kg_P_per_km2_per_y)	0.35	0.08	0.21	0.27	-0.20	0.03	0.13	0.04	0.37	-0.17
Per_area_DOP_(kg_P_per_km2_per_y)	0.03	0.30	-0.01	0.11	-0.17	0.36	-0.03	0.40	0.08	-0.08
Per_area_particulate_P_(kg_P_per_km2_per_y)	0.09	0.05	0.12	0.03	-0.20	-0.07	0.04	-0.03	0.29	-0.16
Per_area_total_P_(kg_P_per_km2_per_y)	0.19	0.10	0.16	0.13	-0.23	-0.01	0.07	0.03	0.35	-0.19
Latitude	0.14	0.20	0.02	0.21	0.40	0.16	0.01	0.04	0.10	0.24
Total_N_deposition_(kg_per_km2_per_y)	0.33	-0.05	0.47	0.02	-0.22	-0.03	0.15	-0.03	0.05	0.02
River_plume_area/COSCAT_area	-0.23	-0.04	-0.23	-0.13	-0.24	0.03	0.04	0.06	-0.19	0.14
Upwelling_(cm/d)	-0.14	-0.08	-0.12	-0.10	-0.06	-0.05	-0.03	-0.03	-0.10	-0.05
Net_N_onwelling_per_unit_area_(kg_N_per_km2_per_yr)	0.02	0.06	-0.10	0.10	0.77	0.04	0.00	-0.03	0.06	-0.09
Submarine_groundwater_discharge_(kg_N_per_km2_per_y)	0.46	-0.02	0.39	0.25	-0.09	-0.03	-0.07	-0.03	0.60	-0.04
Mixed_layer_depth_-_mean	0.53	0.38	0.37	0.52	0.47	-0.03	0.31	-0.11	0.28	-0.22
Mixed_layer_depth_-_closest	0.24	0.21	-0.02	0.39	0.63	-0.05	0.00	-0.09	0.14	-0.19
Mixed_layer_depth_-_composite	0.53	0.38	0.37	0.51	0.48	-0.04	0.31	-0.12	0.27	-0.24
Surface_oxygen_ml/l	-0.03	0.14	-0.16	0.13	0.24	0.19	-0.11	0.09	0.04	0.42

[a] See also Table 5.1.

Total = total of all types;ASP = Amnesic shellfish poisoning; ATE = Aerosolized toxins effects; AZP = Azaspiracid shellfish poisoning; CTE = Cyanobacterial toxins effects; DSP = Diarhetic shellfish poisoning; NSP = Neurotoxic shellfish poisoning; PSP = Paralytic shellfish poisoning; Other = any other bloom type; "0" = type not recorded.

Nutrients show a positive and important influence of occurrences of blooms of all types in the HAEDAT database (Table 5.2). A first conclusion is that mixed layer depth, nutrient availability promote HABs and in conditions of low biomass production HABs occur more frequently than in a high productive environment.

We also use worldwide data for the following species: *Prorocentrum minimum*, *Noctiluca*, *Pseudo-nitzschia* and *Karenia*. The occurrences and ancillary information such as length of bloom and extent were collected from literature, reports and other sources. The data is provided by the Scientific Committee on Ocean Research (SCOR) / Land-Ocean Interactions in the Coastal Zone (LOICZ) workgroup 132 on "Land-based Nutrient Pollution and the Relationship to Harmful Algal Blooms in Coastal Marine Systems". Furthermore, data was collected from the State Oceanic Administration China People's Republic (SOA, 2014) on algal bloom occurrences in Chinese coastal seas during the period 1990-2013 (Figure 5.4).

It is not known if the observations in the Chinese data are duplicating the HAEDAT data . However, it is clear that a number of observed blooms in the data collected by SCOR 132 are not in the HAEDAT database, for example in the Arctic Ocean, Southeast Asia, Subsaharan Africa, parts of South America and even in North America observed bloom events are not in the HAEDAT data.

The HAEDAT data suggest a recent decreasing trend in the number of observed HABs. We do not know if this is related to a delay in entering such events in the database, or a deceasing interest or effort by countries, or an actual downward trend in bloom events. With the acceleration of nutrient use in agriculture and increasing urbanization, we think the latter is not the case.

The HAEDAT database contains information based on yearly national reports by ICES and PICES member states. The available information on individual events varies greatly from event to event or country to country. Monitoring intensity, number of monitoring stations, number of samplings, stations, etc. also varies greatly and therefore there is not a direct proportionality between recorded events and actual occurrences of e.g. toxicity in a given region. Furthermore, areas with numerous recorded occurrences of HABs, but with efficient monitoring and management programs, may have very few problems and a low risk of HAB-related toxic events, whereas rare HABs in other areas may cause severe problems and represent significant health risks.

5.3. Impacts on fisheries

Model output was collected for 70 coastal systems where Ecopath and EcoSim models (Christensen and Walters, 2004) have been run (Figure 5.5). We have begun to

use this information in conjunction with estimates of coastal nutrient loading to develop relationships between fishery production and potential controlling variables such as nutrient inputs and hypoxia. Depending on the strength of these relationships, they may or may not be used to make global-scale estimates of anthropogenic impacts on fisheries at the global scale.

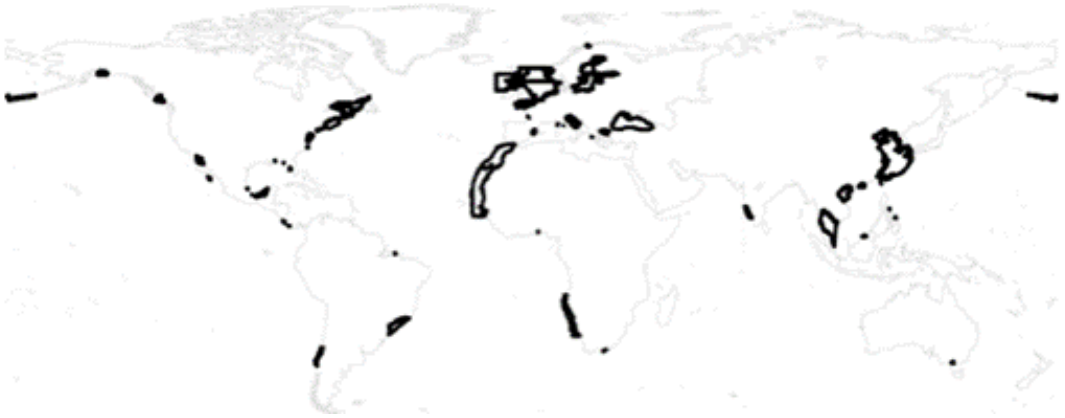

Figure 5.5. Location of HYPOFIN systems (systems for which Ecopath or Ecosim models have been run)

6. Enhance predictive capability of models

Activities regarding enhancement of our models focused on improving the Global NEWS river nutrient export models (section 6.1). In addition to these, we also developed a new coastal model to estimate the biogeochemistry of coastal waters and impacts on oxygen availability (section 6.2). Data from the SCOR/LOICZ HAB work group, HAEDAT and observations collected by (SOA, 2014) will be used in conjunction with information about HAB risk indicators such as the ICEP indicator to develop quantitative models predicting the probability of HAB occurrence as a function of nutrient loads and sources (section 6.3). Initial analysis of nutrient impacts on fisheries is presented in section 6.4.

6.1. River export models

Two NEWS sub-models have been substantially enhanced since the publication of the NEWS-2 models (Mayorga et al., 2010). The NEWS-DIP submodel has been evaluated and applied at 0.5 degree resolution, substantially enhancing its spatial resolution over prior implementations (Figure 6.1). To enhance the temporal resolution of nutrient transport predictions beyond what was possible in the original Global NEWS models, a seasonal version of the NEWS-DIN model was developed and published (McCrackin et al., 2014; Figure 6.2). NEWS-DIN and NEWS-DON were also downscaled and applied to the Continental US, using US-specific N loading databases (McCrackin et al., 2013, 2015; Figures 6.3 and 6.4). The US-specific implementation of NEWS-DIN was used to perform a multi-model comparison of source attribution for the US (Figure 6.4) and to examine potential trajectories of change in dissolved N loading to the US coast (Figure 6.3). Prior to these efforts, all NEWS models could only be used to make predictions of annual average nutrient flux at the scale of basins with more than 10 half-degree cells.

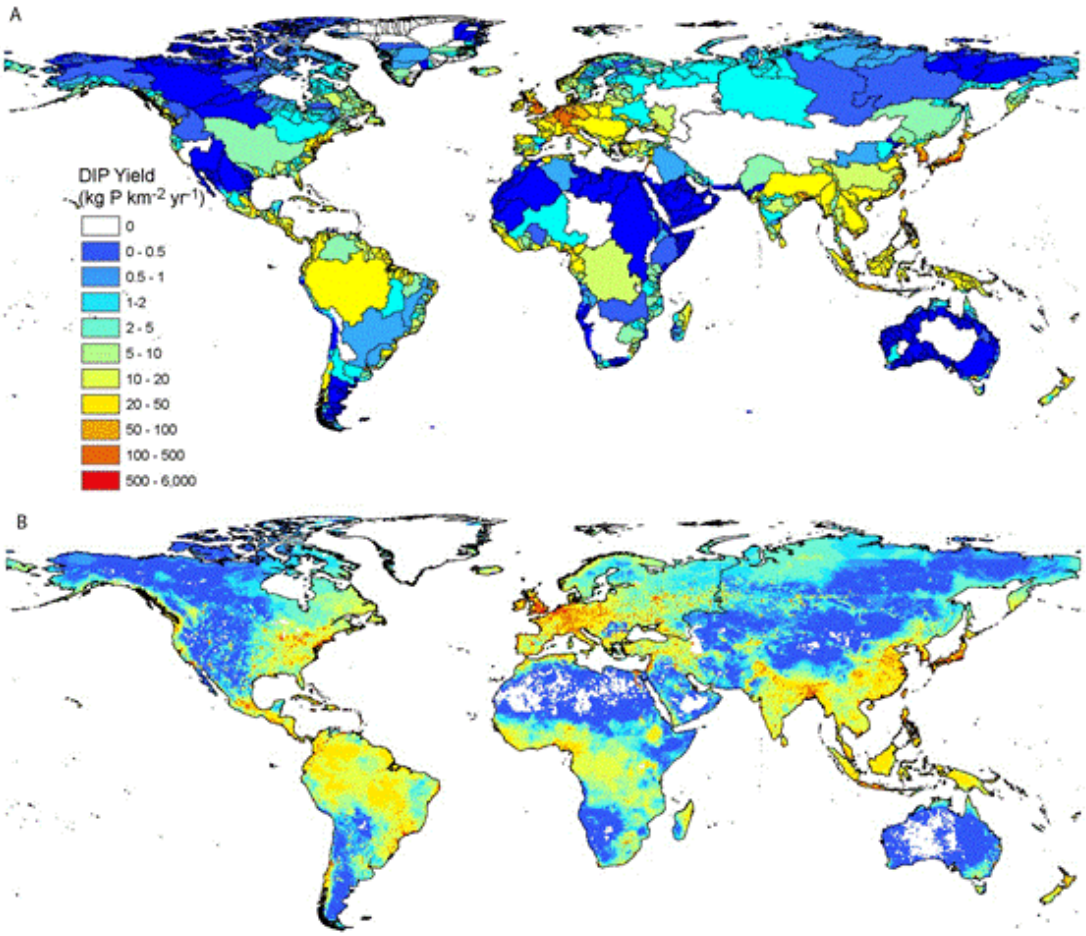

Figure 6.1. Comparison between the basin-scale NEWS-DIP submodel (A) and a half-degree implementation of a revised NEWS-DIP model called NEWS-DIP-Half-Degree (Harrison et al., 2010b).

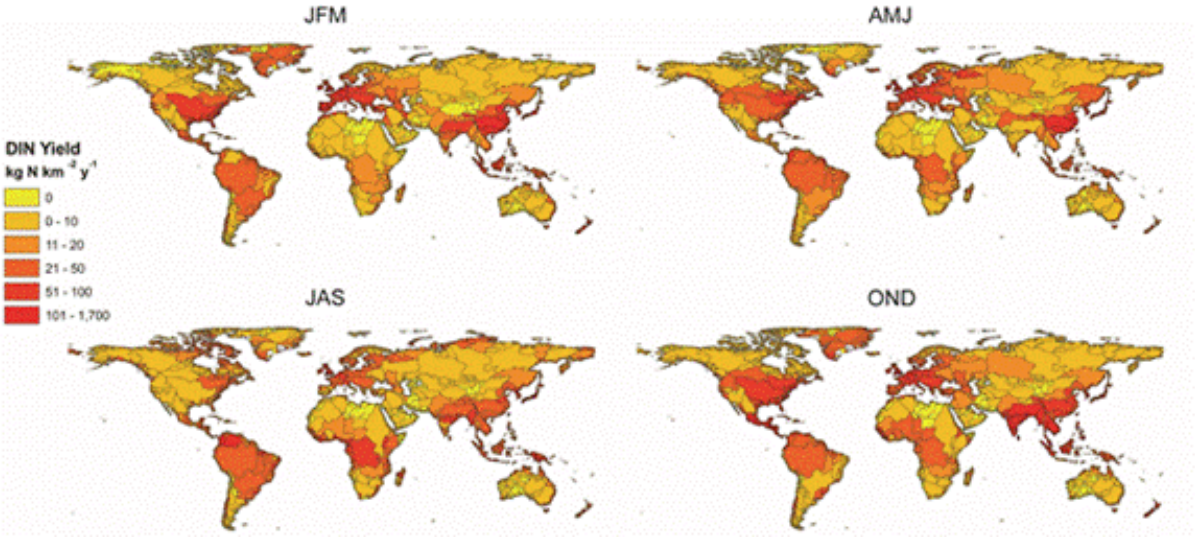

Figure 6.2. Predictions of DIN yield based on a seasonal implementation of the NEWS-DIN model (McCrackin et al., 2014).

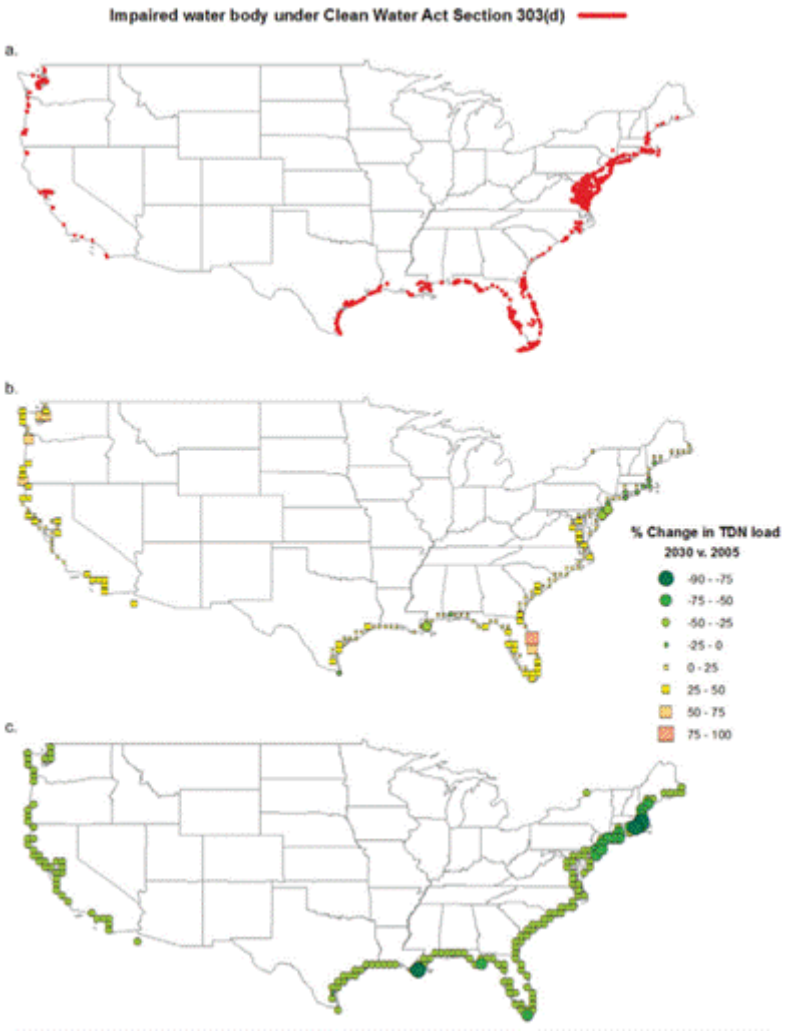

Figure 6.3. (a) Red lines indicate coastal areas identified as impaired due to nitrogen concentrations, algal growth, noxious aquatic plants, or oxygen depletion under Section 303(d) of the Clean Water Act. Symbols are percentage change in NEWS2US-TDN-derived loads at river mouths between 2005 and 2030 for (b) Business as Usual and (c) Ambitious scenarios (yellow square = increase between 2005 and 2030; green circle = decrease). Source: McCrackin et al (2015).

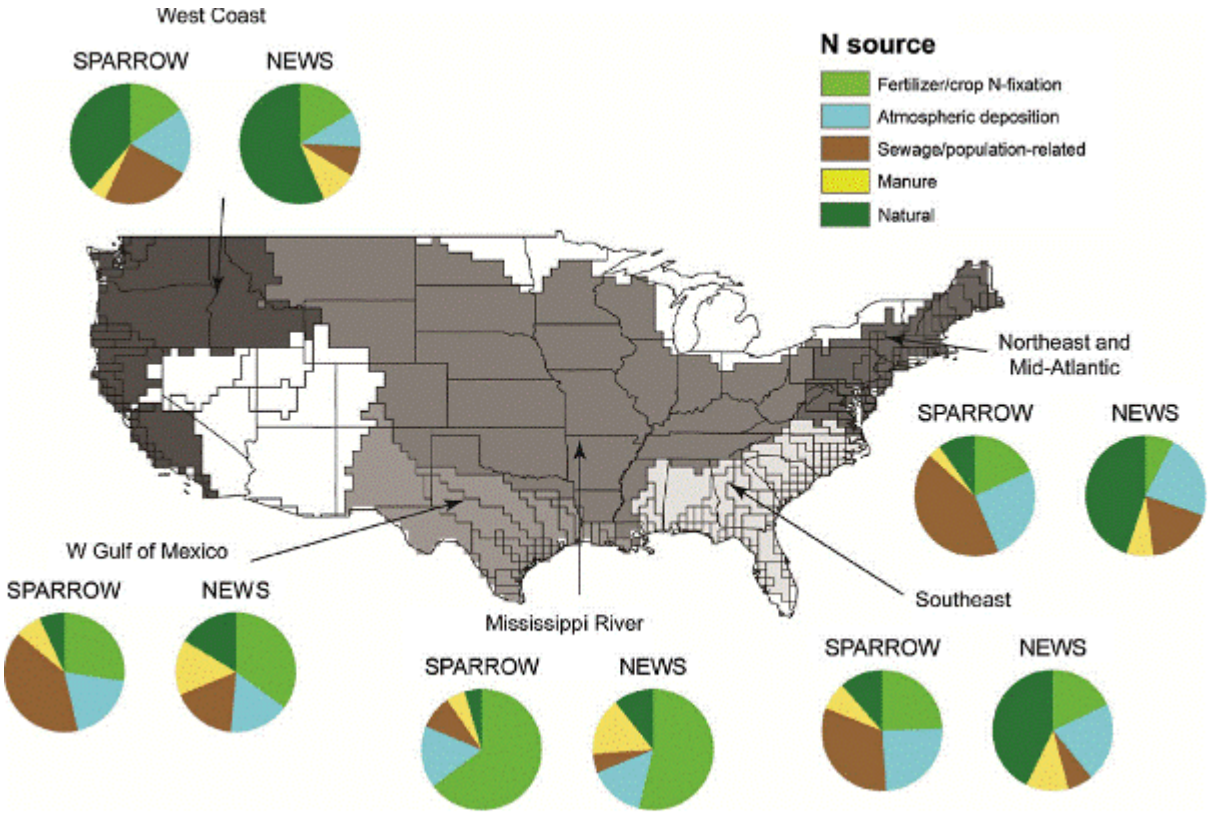

Figure 6.4. Comparison of N source attribution between SPARROW and NEWS models for regions of the US. White areas were not included in the comparison. Source: McCrackin et al. (2013).

6.2. Hypoxia

OXYGEN DEPLETION HAS A PROFOUND EFFECT ON AQUATIC ECOSYSTEMS, ALTERING THE STRUCTURE AND FUNCTION OF NATIVE COMMUNITIES (RABALAIS, 2002) AND PERTURBING GEOCHEMICAL DYNAMICS (MIDDELBURG AND LEVIN, 2009). AS A RESULT, THERE IS MUCH INTEREST IN DEVELOPING REMEDIATION STRATEGIES FOR THESE SO-CALLED "DEAD ZONES" (DÍAZ ET AL., 2009). TO BE ABLE TO EVALUATE THE EFFECTIVENESS OF POTENTIAL MITIGATION SCHEMES, IT IS IMPORTANT TO BE ABLE TO QUANTITATIVELY LINK HUMAN CAUSES WITH THEIR CORRESPONDING EFFECTS IN THE MARINE REALM. WITH THIS GOAL, WE HAVE DEVELOPED AND ARE IN THE PROCESS OF PREPARING FOR PUBLICATION THE COASTAL OCEAN OXYGEN LINKED TO BENTHIC EXCHANGE AND NUTRIENT SUPPLY (COOLBEANS) MODEL, A NEW APPROACH CONNECTING CHANGES IN NUTRIENT LOADING TO SHIFTS BOTTOM WATER OXYGEN THROUGHOUT THE GLOBAL COASTAL OCEAN. OXYGEN CONCENTRATIONS IN DEEP WATERS REFLECT THE BALANCE BETWEEN OXYGEN SUPPLY BY PHYSICAL PROCESSES AND OXYGEN UPTAKE BY BIOGEOCHEMICAL PROCESSES. THE LATTER IS ULTIMATELY DRIVEN BY THE MINERALIZATION OF ORGANIC MATTER DEPOSITED FROM OVERLYING WATERS. CONSEQUENTLY, THE MODEL PRESENTED HERE CONSIDERS THREE PROCESSES:

- VENTILATION OF DEEP WATERS
- DIAGENETIC OXYGEN CONSUMPTION
- TRANSLATION OF NUTRIENT LOADING INTO DEPOSITIONAL FLUXES OF ORGANIC MATTER (FIGURE 6.5)

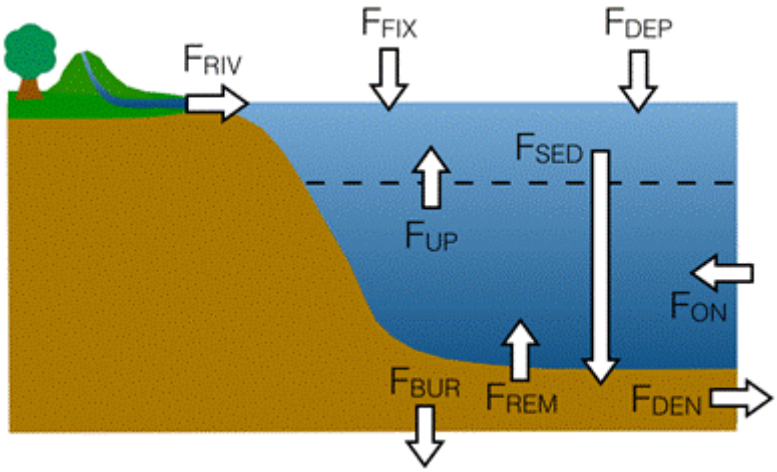

Figure 6.5. Scheme of the nutrient mass-balance scheme used to parameterize COOLBEANS. All fluxes refer to nitrogen (N) and are defined as follows: F_{RIV} riverine input, F_{FIX} nitrogen fixation, F_{DEP} atmospheric deposition, FON onwelling, FDEN diagenetic denitrification, FBUR burial, FREM remineralisation other than denitrification, F_{SED} export of organic matter to sediments, and F_{UP} upwelling. The dashed line represents the pycnocline.

BENTHIC OXYGEN DEMAND

In the deep ocean, benthic oxygen demand (BOD) is chiefly due to aerobic respiration (Soetaert et al., 1996), which consumes the vast majority of organic matter that reaches the seafloor (Middelburg et al., 1997). Consequently, BOD has previously been used as a proxy for the depositional flux of organic matter (Andersson et al., 2004). In coastal waters, however, the link between organic deposition and BOD is more complex. First, the burial efficiency of organic matter in the coastal ocean is much higher than for sediments in the deep ocean. Next, organic matter that is re-mineralized in coastal sediments is not only decomposed via aerobic respiration, but through numerous other pathways (e.g., iron reduction, denitrification, sulfate reduction). As a result, the majority of oxygen that is consumed in coastal sediments is due to the oxidation of reduced species produced by these pathways (e.g., Fe^{2+}, NH_4^+, HS^-) rather than aerobic respiration.

Through a combination of empirical relationships, COOLBEANS accounts for this myriad of biogeochemical processes that affect BOD. Specifically, the model considers organic carbon burial and remineralization, coupled nitrification-denitrification, iron and sulfate reduction, and pyrite burial. In addition, water column supported denitrification is included and estimated by fitting the BOD model to a previously published database, although it plays a minor role in BOD.

The database used to calibrate and assess the skill of the benthic oxygen demand model was compiled by Borsuk et al. (2001). There are 66 instances included within the database from sites throughout the coastal ocean (Figure 6.6) with each instance including water depth, benthic oxygen demand, and annual organic carbon loading (defined as net primary production plus external inputs). These data are supplemented with the average annual bottom water temperatures in the region, as determined by from the World Ocean Atlas (NOAA, 2009).

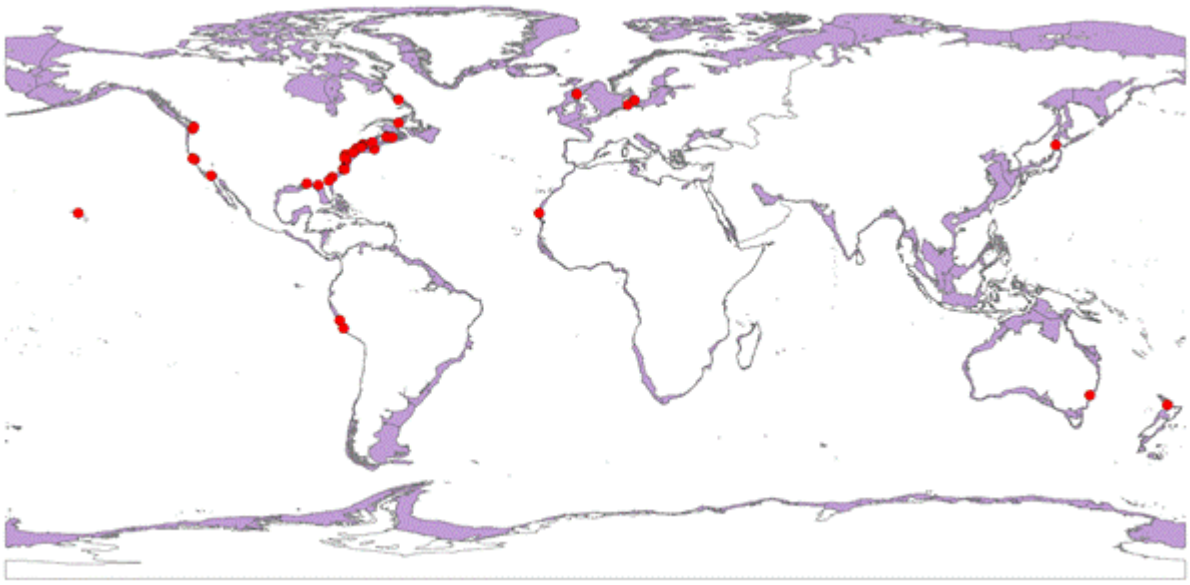

Figure 6.6. Locations of sites from Borsuk et al. (2001) that are used to calibrate the benthic oxygen demand model.

PHYSICAL OXYGEN SUPPLY

To estimate vertical exchange between surface and deep waters, we assume that COSCAT oxygen concentrations are currently stable and, therefore, benthic oxygen demand is met by physical supply. The following equation states this balance mathematically:

$$\frac{\mathrm{DC}}{\mathrm{DT}} = \alpha(\mathrm{C}_0 - \mathrm{C}) - \frac{\mathrm{BOD}}{\mathrm{L}} = 0 \quad (1)$$

where C denotes bottom water oxygen concentration (MOL M^{-3}), C_0 represents surface water oxygen concentration (MOL M^{-3}), α denotes the exchange coefficient (Y^{-1}). BOD is benthic oxygen demand (MOL M^{-2} Y^{-1}), t is time (Y), and L is the thickness of the deep water layer considered. The first term, $\alpha(\mathrm{C}_0 - \mathrm{C})$, represents a simple parameterization of oxygen supply, whereas the second term, $\left(\frac{\mathrm{BOD}}{\mathrm{L}}\right)$, accounts for oxygen uptake by sediments over a layer of thickness L. Here, we consider a 1 m layer overlying sediments. Assuming steady-state $\left(\text{I. E., } \frac{\mathrm{DC}}{\mathrm{DT}} = 0\right)$, exchange between

surface and deep waters — denoted here as α — can be estimated as all other values are known.

NUTRIENT MASS BALANCE

Changes in nutrient loading alter the balance between oxygen supply and demand by enhancing net primary production and, consequently, organic matter export to sediments. In turn, this increases benthic oxygen uptake. In COOLBEANS, this is modeled by constructing a nutrient budget (Figure 6.5) that furnishes the change in organic matter export with respect to changes in nutrient loading. This is translated into an elevated oxygen demand by means of the BOD component of the model and changes in bottom water oxygen are calculated using equation 1.

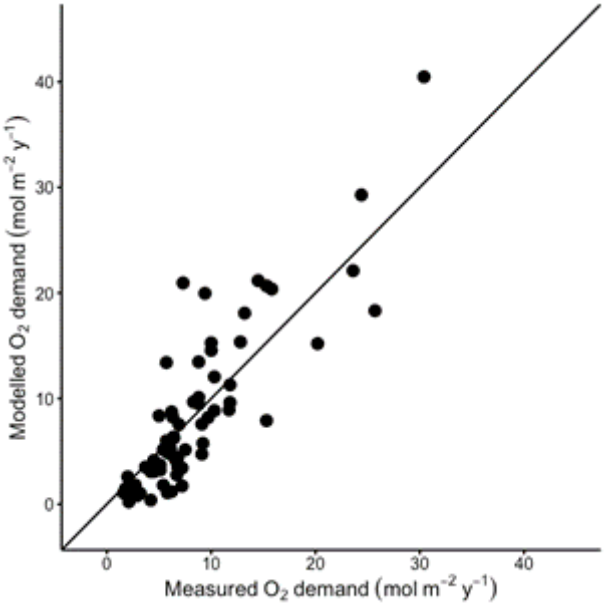

Figure 6.7. A comparison of modelled versus observed benthic oxygen demand. The 1:1 line represents a perfect agreement between model and observation. The Nash-Sutcliffe model efficiency coefficient is 0.51.

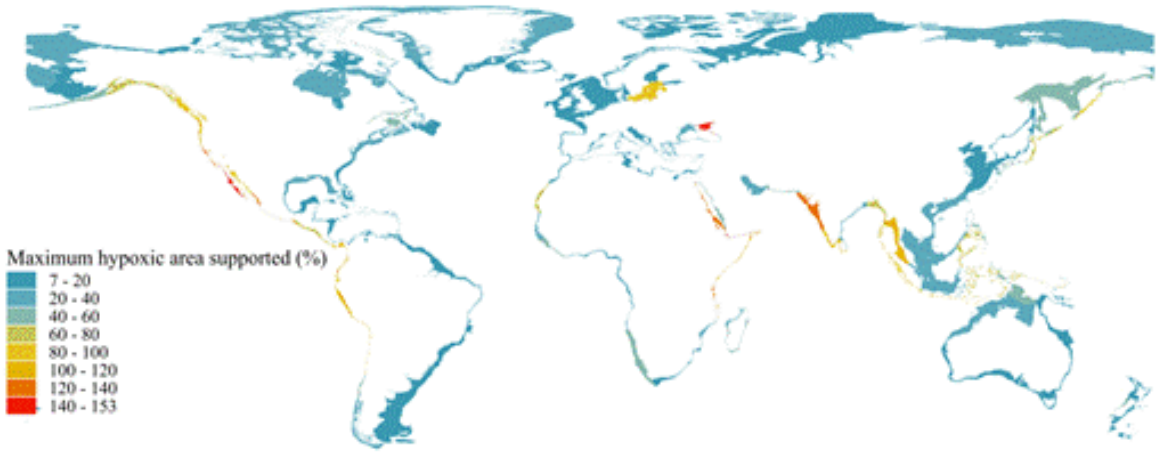

Figure 6.8. Map showing the maximum hypoxic area supported by present day nutrient loads as a percent of the biogeochemically active region.

APPLICATION

The generic COOLBEANS model is applied to the entire global coastal ocean, which is divided into 152 COSCAT segments (Table 4.1), that are small enough to be meaningful yet large enough to be manageable. So far, the COOLBEANS model appears to do well in predicting sediment O2 demand (Figure 6.7).

We are now confident to apply COOLBEANS to examine patterns of sensitivity in coastal systems to changes in nutrient loading (Figure 6.8). The model yields a good agreement with the observed hypoxia events presented in Figure 5.1, for example in the Baltic Sea, West and East U.S.A.

6.3. HABs

Nutrients can stimulate or enhance the impact of toxic or harmful algal species in several ways (Anderson et al., 2002). At the simplest level, harmful phytoplankton may increase in abundance due to nutrient enrichment, but remain in the same relative fraction of the total phytoplankton biomass. Even though non-HAB species are stimulated proportionately, a modest increase in the abundance of a HAB species can promote noticeable differences in the ecosystem because of its harmful or toxic effects; more frequently, a species or group of species dominates in response to nutrient enrichment or a change in the ratios of nutrient enrichment (Glibert et al., 2010). Profound changes in the structure of food webs are often observed as a result of eutrophication in coastal marine ecosystems, with changes in the structure of the benthic communities (Lim et al., 2006) and a decline in zooplankton affecting commercial fish production (Rousseau et al., 2000). It is now recognized that these phenomena are not only caused by nutrient enrichment of the marine system per se, but rather by the changes in nutrient stoichiometry.

The Redfield atomic ratio (C:N:P:Si = 106:16:1:20) is a generalized representation of the approximate nutrient requirement of marine diatoms. Coastal enrichment with nutrients, delivered in proportion to diatom demand (Redfield et al., 1963) can stimulate algal production and that of other plants, and in case of high biomass blooms leads to eutrophication problems such as hypoxia. However, when nitrogen (N) and phosphorus (P) are discharged to coastal waters in excess over silicon (Si) with respect to the requirements of diatoms, diatom growth can be limited, and blooms of non-diatom phytoplankton, often undesirable algal species (harmful algae), may develop instead.

The Index for Coastal Eutrophication Potential (ICEP) is an indicator for the potential of riverine nutrient export to sustain new production of non-diatoms phytoplankton biomass; it is calculated by comparing the N, P and Si loading to the Redfield ratios expressing the requirements of marine diatoms growth. A negative value of the ICEP indicates that Si is present in excess over the other nutrients and would thus indicate a low likelihood of HAB development. Positive values of ICEP indicate an excess of N or P over Si, which may lead to blooms of non-diatom, possibly harmful algae species. The ICEP represents the potential impact of the riverine delivery to the coastal zone. ICEP does not take into account the particular morphological, climatic and hydrological conditions such as stratification, and the impact of upwelling of nutrients that locally determine the response of the marine algae in the receiving coastal zone (GEOHAB, 2006).

Global NEWS river nutrient export (see Chapter 2) for 2000, 2030 and 2050 (representing AM and GO scenarios) was used to calculate ICEP values for more than 6000 river basins globally to assess the potential risk that non-diatom algal growth may lead to harmful algal blooms in coastal marine ecosystems. The model used to estimate river export of N and P from point sources (sewage) and nonpoint sources (agriculture and natural ecosystems) combined with Global NEWS data for dissolved silica (DSi) presented by Beusen et al. (2009).

ICEP is calculated on the basis of riverine N, P and Si deliveries, allowing to determine the possible problems resulting from a new production of non-siliceous algae sustained by external inputs of N and/or P brought in excess over silica, i.e., in limiting conditions for the diatom growth. Compared to N:P ratios which are often considered (e.g. Glibert et al., 2008), the ICEP adds information about the role of Si in determining potential eutrophication impacts of changing element stoichiometry. ICEP represents the new production of non-siliceous algal biomass potentially sustained in the receiving coastal water body by either nitrogen or phosphorus delivered in excess over

silica. ICEP is based on the Redfield atomic C:N:P:Si ratio 106:16:1:20 (Redfield et al., 1963). The molar weights of these elements are 16, 14, 31 and 28.

ICEP is calculated as follows:

$$\text{For } \frac{\text{TN(river)}}{(14*16)} > \frac{\text{TP(river)}}{31}:$$

$$\text{ICEP(river)} = \left(\frac{\text{TN(river)}}{(14*16)} - \frac{\text{DSi(river)}}{(20*28)} \right) *106*12/365$$

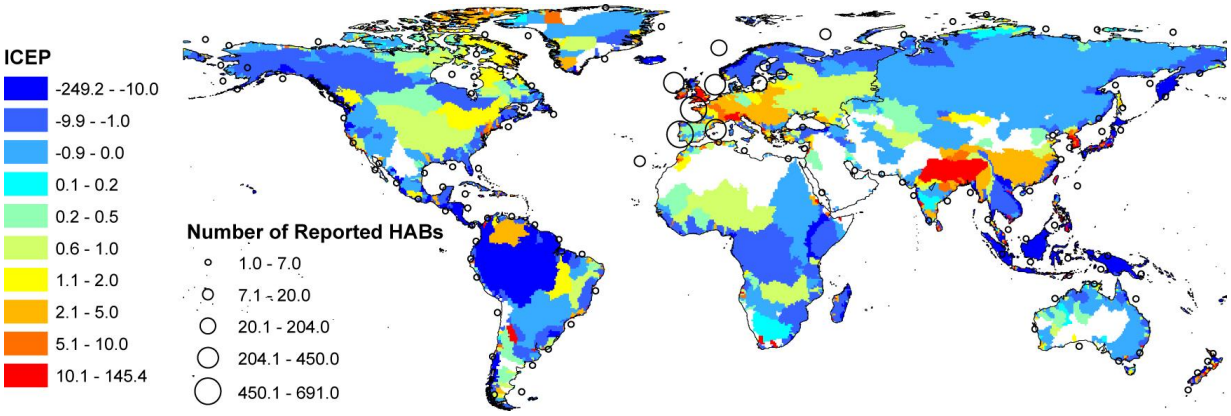

Figure 6.9. Calculated Index for Coastal Eutrophication (ICEP) of water draining into coastal seas presented on the scale of river basins, and observed algal blooms collected from HAEDAT.

$$\text{For} \frac{\text{TN(river)}}{(14*16)} \leq \frac{\text{TP(river)}}{31}$$

$$\text{ICEP(river)} = \left(\frac{\text{TP(river)}}{31} - \frac{\text{DSi(river)}}{(20*28)} \right) *106*12/365$$

These equations can be applied using concentration (mean annual concentration g m^{-3}) or total loads (kg yr^{-1}). The above equations have been used to compute the ICEP for global river basins using the Global NEWS data presented in Chapter 2 (Figure 6.9). The results for 2000 show an agreement between positive ICEP values and observed HABs (Figure 6.9). Local physical and environmental conditions will, apart from the nutrient loading and element ratios used in the ICEP concept, determine the propensity of a coastal marine ecosystem for developing high biomass algal blooms, harmful algal blooms or hypoxia.

For example, the observed HABs in Indonesian seas as collected by SCOR 132 are not in the HAEDAT data. They may be more related to natural phenomena such as upwelling than to river nutrient export. Upwelling off the coasts of Java-Sumatra and Banda Sea/Irian Jaya coast show that they are mostly forced both locally by the alongshore winds associated with the SE monsoon and remotely by atmosphere-ocean circulation associated with El Niño Southern Oscillation (ENSO) (e.g. Gordon et al., 2010).

6.4. Fisheries

Elevated nutrient loading has been associated with elevated fish production, up to a point (Nixon and Buckley, 2002). However, after a threshold has been reached, it has been hypothesized that hypoxia leads to declines in fisheries production (Breitburg et al., 2009). Our first-cut efforts to link coastal nutrient loading with fish production (Figure 6.10), suggest a weak positive relationship ($P<0.001$, $R^2 = 0.21$) between N loading and mobile consumer (fish and decapod) biomass, with little evidence of decreasing biomass at the highest rates of nutrient loading. However, these results are highly provisional.

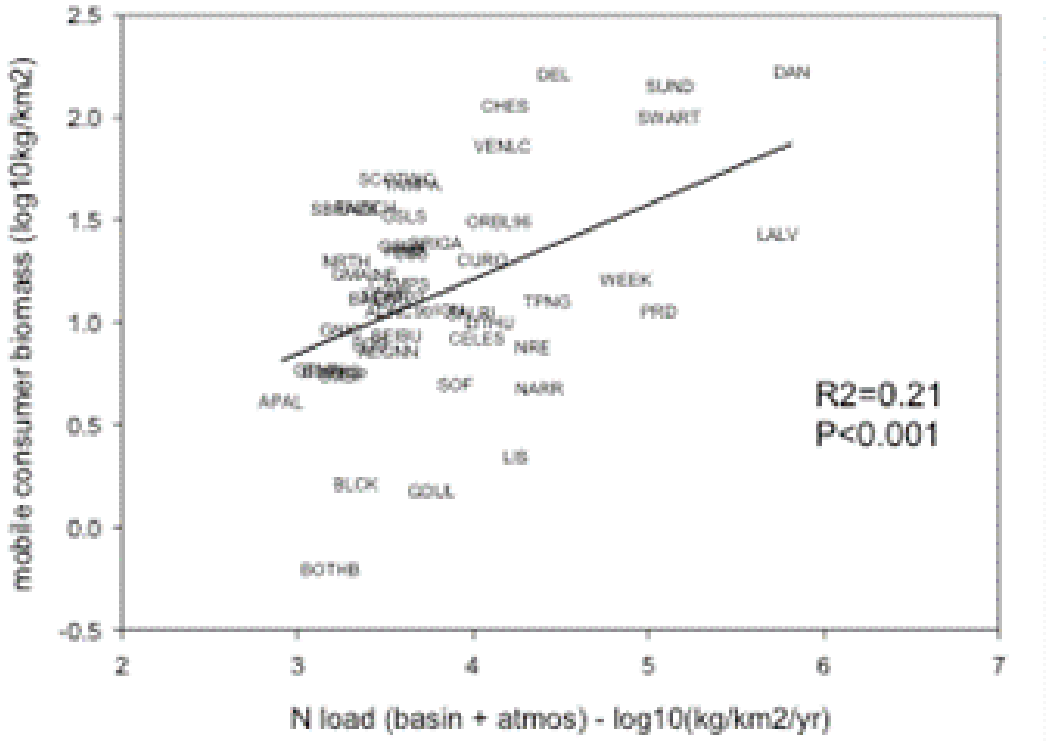

Figure 6.10. The relationship between log N loading to coastal regions and log fish biomass for 70 HYPOFIN regions.

7. Assessment of effects of nutrient loading

7.1. Analysis and maps of past, current and future contributions of different nutrient sources

Past trends in river nutrient export

Global trends in nutrient export by rivers are the result of changes in human activities and hydrology. The increased river export of DIN for the period 1970-2000 at the global scale is primarily caused by increasing food production, particularly increased N inputs due to fertilizer use and animal production. Wastewater and atmospheric nitrogen deposition stemming from agriculture, energy and industry contribute to a lesser extent to the increased river DIN export (Figure 7.1). Increases in river export of DIP can be explained by increased inputs of P to rivers largely from wastewater and to a lesser extent from food production (Figure 7.1). Increasing river export of particulate forms of N and P is a result of soil loss due to erosion and land use change. This not only holds for particulate forms of P and P, but also of C. River export of particulate N, P and C is not as large as one would expect from erosion trends alone because of sediment trapping in reservoirs, thus reducing their transport to coastal waters.

Global river export of all forms of N and P (and C) increased during the period between 1970 and 2000 (Figure 7.2), although the forms responded differently. Large increases (30%) occurred for dissolved inorganic N and P, while particulate loads increased by only about 10%. The increase of dissolved organic nutrients was much less (<5%). Total N (DIN + DON + PN) river export increased from 37 to 43 Tg between 1970 and 2000. The Global NEWS estimate for 1970 agrees fairly well t with the estimated TN river export for 1970 based on an extrapolation of measurements for world rivers by Meybeck (1982). This increase in TN is largely the result of a 35% increase in DIN export from 14 to 19 Tg N per year. Close to 40% of the total N in river export is DIN.

The 29% global increase between 1970 and 2000 for DIP is similar to that of DIN (Figure 7.1). Looking at the different forms of P, we see that the largest absolute increase in P load is caused by particulate P (13% between 1970 and 2000). This is because particulate P is the dominant form (5.9 Tg P in 2000) of total P export of 7.6 Tg P per year in 2000 by world rivers. Global NEWS model estimates for 1970 for DIN and DON (14 and 10 Tg N per year, respectively) and dissolved P (1.7 Tg P per year) agree with estimates for global river export for 1970 by Meybeck (1982) (12 Tg DIN-N, 10 Tg DON-N and 2 Tg dissolved P per year). Our estimates for PN and PP (12 Tg N and 6 Tg P per year) are considerably lower than Meybeck's (21 Tg N and 20 Tg P per year), which were based on a POC budget and assumed fixed N: C : P ratios. The Global NEWS model estimates for PN and PP are derived from Total Suspended Solids in rivers, which is more reliable than Meybeck's extrapolation on the basis of a few measurements.

There are large differences between world regions. In Europe and North America small increases in river DIN export were calculated between 1970 and 2000 (Figure 7.1). In Europe and North America wastewater is the single largest source of DIP river export in all years and scenarios. In Europe there has been a rapid decrease in DIP export between 1970 and 2000, mainly due to an increase of the use of P-free detergents and an increase of P removal in wastewater treatment facilities.

In South Asia, increasing DIN and DIP river export (79% and 120% increases for 1970-2000 for DIN and DIP, respectively) are associated with increased use of N and P fertilizers and manure application to sustain crop growth and to increased inputs of human wastewater to surface water (Figure 7.1).

In South America, recent increases in coastal loading of DIN and DIP have not been as large as in South Asia, and seem to be linked to growing rates of N fertilizer application and increased wastewater discharge to surface waters, and increases in manure production (Figure 7.3). Africa and South America have primarily low to medium income countries and show similar relative contributions of watershed N sources to DIN export for 1970 and 2000 (Figure 7.4).

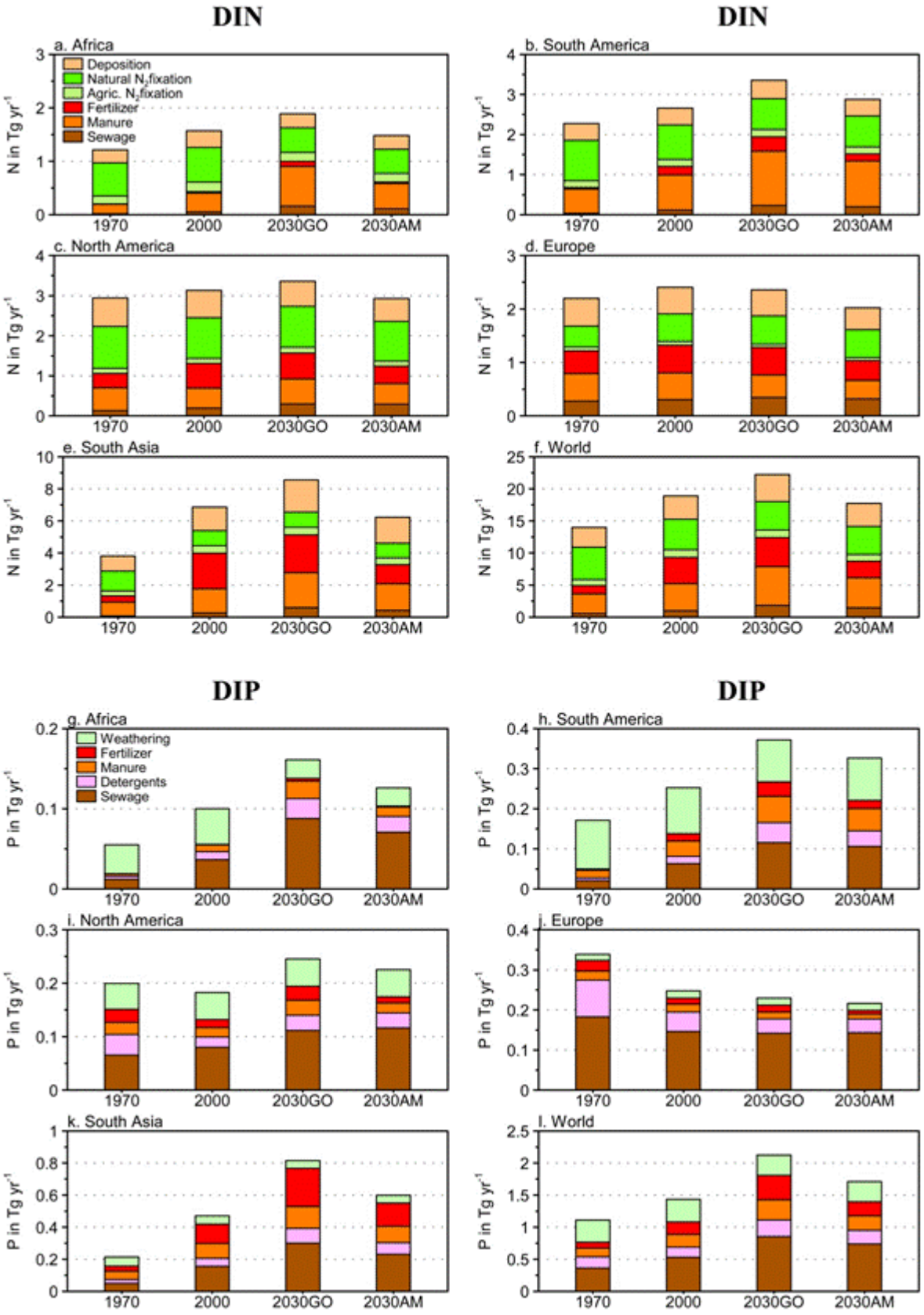

Figure 7.1. Model-predicted contribution of: nitrogen sources in watersheds to DIN river export (panels a-f), and phosphorus sources in watersheds to DIP river export (panels g-l), for various world regions. Figure reprinted from Seitzinger et al. (2010c).

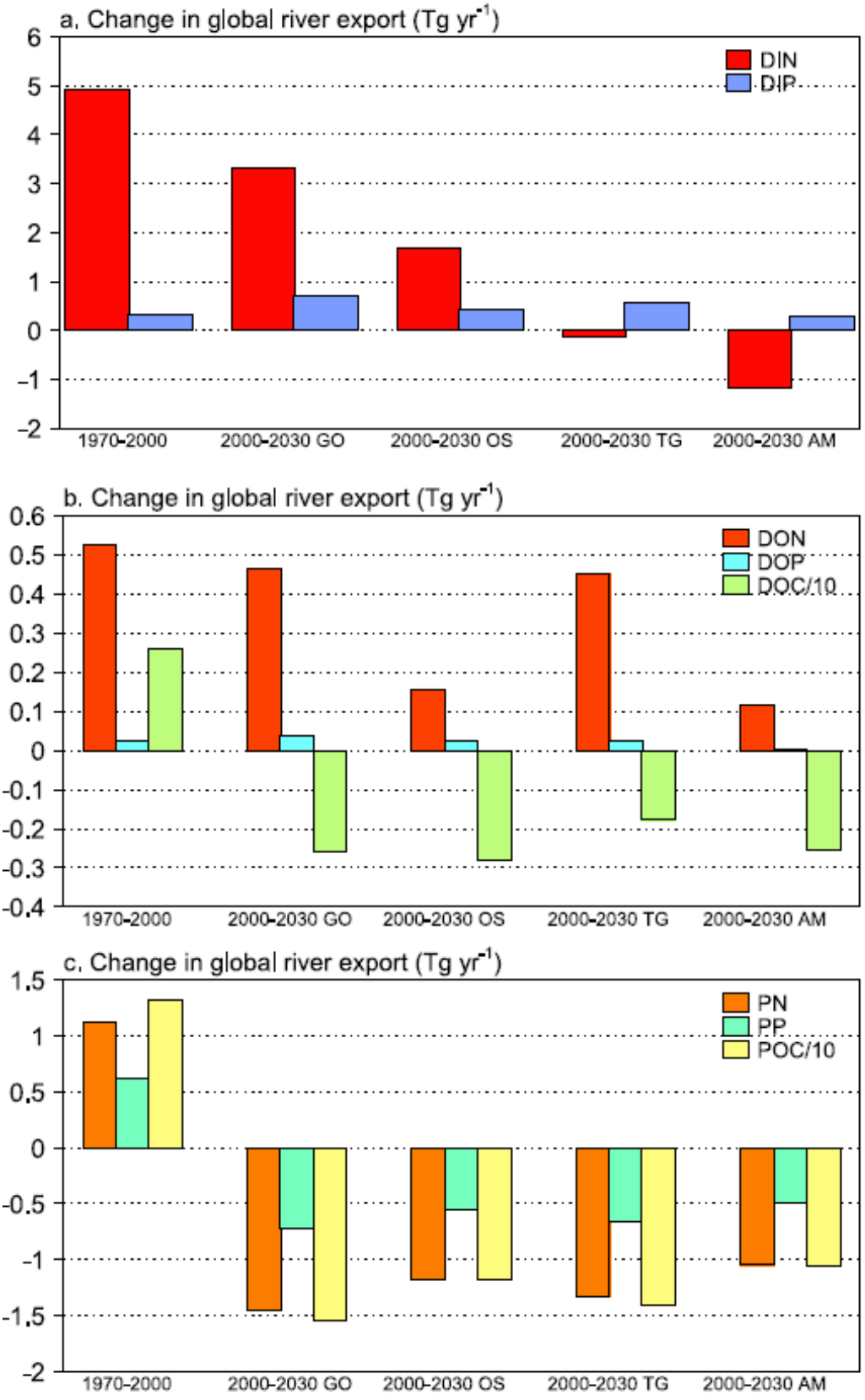

Figure 7.2. Change in river export of dissolved inorganic N (DIN) and P (DIP) to coastal waters between 1970 and 2000, and between 2000 and 2030 for the four MEA scenarios (top), change of river export dissolved organic nutrients (DON, DOP, DOC)

(middle) and change in river export of particulate nitrogen (PN), particulate phosphorus (PP) and particulate organic carbon (POC) (bottom). Note differences in scales. Units: Tg N, P or C yr^{-1}. Figure reprinted from Seitzinger et al. (2010c).

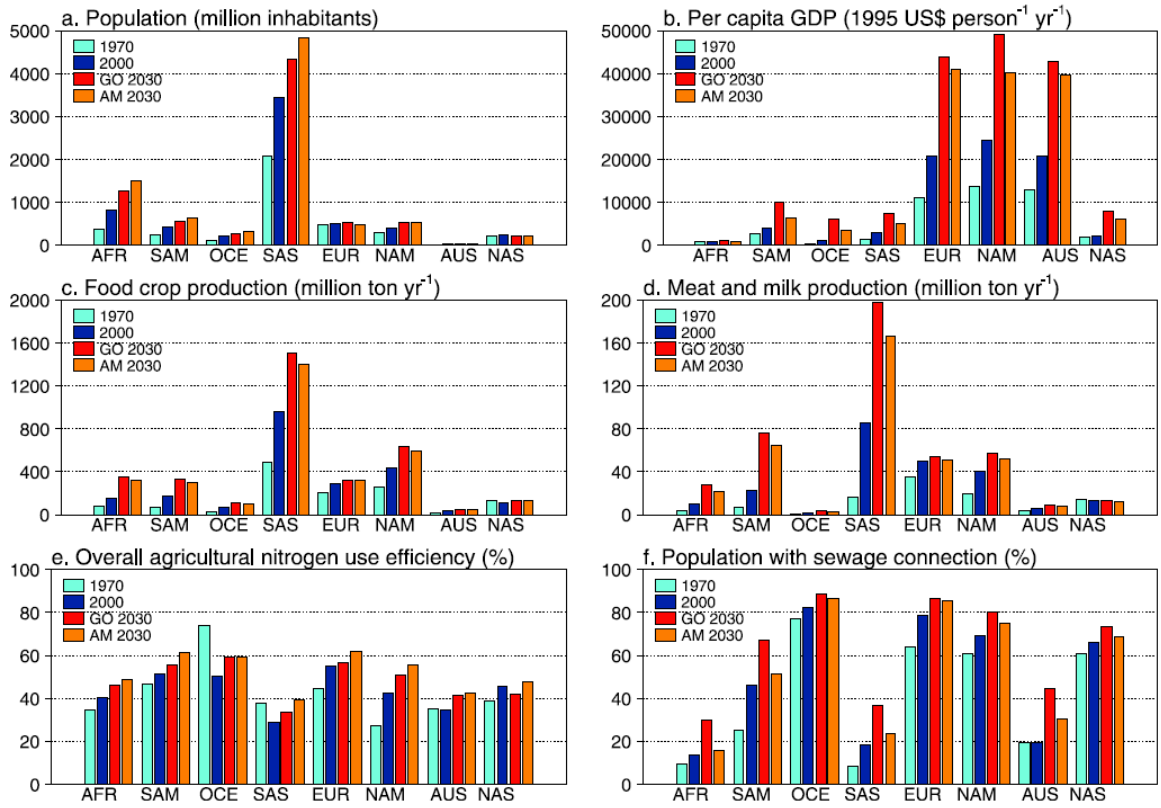

Figure 7.3. Anthropogenic drivers of nutrient flows for 8 world regions for 1970, 2000, and for 2030 for the Global Orchestration (GO) and Adapting Mosaic (AM) scenarios. Data taken directly from MEA (Alcamo et al., 2006) on the scale of 24 world regions include: a) population, b) per capita gross domestic product, c) crop production expressed as dry matter; d) meat and milk production in dry matter. Values computed in this study, used as indirect drivers, include: e) the percentage of the population with a sewage connection from Van Drecht et al. (2009); and f) overall agricultural efficiency (including crop and livestock production systems) of nitrogen use from Bouwman et al. (2009); this efficiency is from a surface balance perspective, ignoring imports and exports of fertilizers, feedstuffs, agricultural products, and other N- and P-bearing materials. Figure reprinted from Seitzinger et al. (2010c).

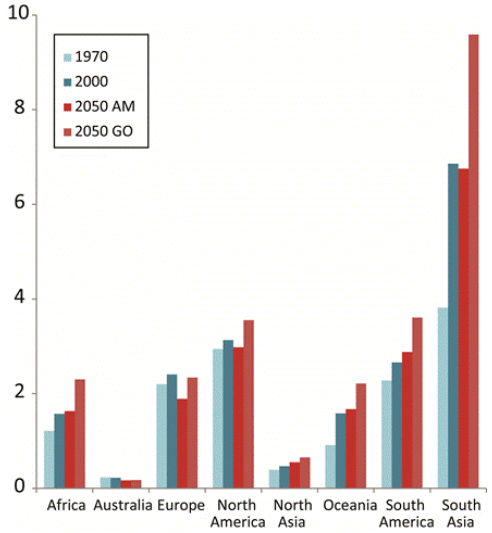

Figure 7.4.Historic and model-estimated future changes in DIN loading to coasts by major world region under two different Millennium Assessment scenarios: Global Orchestration (GO), and Adapting Mosaic (AM).

In Africa and South America the N mobilization caused by biological N_2 fixation in natural ecosystems plus manure account for about two thirds of DIN export, but their relative contributions change over time. Biological N_2 fixation in natural ecosystems was the single largest source of DIN in river water in 1970, but its relative share decreases due to increasing anthropogenic sources. Wastewater was not a major source of river DIN and DIP in Africa and South America in the past 30 years (Figure 7.1), although locally it may be dominant.

There are large differences in DIP and DIN river export both in the sources, and in the patterns among the continents. Wastewater was a much more important contributor to DIP than to DIN river export in 1970 as well as in 2000 for all continents and scenarios (Figure 7.1). Wastewater has even been the single largest source of DIP river export in all years and scenarios in North America and Europe. In Europe there was a substantial decrease in DIP export from 1970 to 2000, primarily due to an increase of the use of P-free detergents and increased connection to wastewater treatment facilities and more efficient P removal.

General aspects of the scenarios used

Four Millennium Ecosystem Assessment (MEA) scenarios were implemented to analyze possible future trends in coastal nutrient delivery. The MEA scenarios are based on storylines and changes of the main anthropogenic drivers (population, economic growth and food production (Alcamo et al., 2006) (Figure 7.3). Apart from population and economic growth, food consumption and production (Figure 7.4) and trade, the MEA scenarios differ in terms of environmental management (pro-active or reactive) and in the degree and scale of connectedness among and within institutions across country borders (globalization or regionalization).

Scenarios called “Technogarden” and “Adapting Mosaic” were developed assuming pro-active environmental management, while scenarios called “Order from Strength” and “Global Orchestration” assume re-active environmental management. Global Orchestration and Technogarden reflect trends towards globalization, while regionalization is assumed in Order from Strength and Adapting Mosaic. This report focuses on Global Orchestration and Adapting Mosaic, two contrasting scenarios that are often selected as business as usual scenarios.

The MEA storylines and scenarios do not include descriptions of sewage connection and wastewater treatment and nutrient management in agriculture. The storylines were therefore translated four quantitative nutrient management scenarios consistent with the general idea of the scenarios and the anthropogenic drivers (Bouwman et al., 2009).

For example, in Technogarden and Global Orchestration, the gap between full connectivity to sewage systems and advanced treatment will be closed much more rapidly than in Adapting Mosaic and Order from Strength, and similarly, fertilizer use in developing countries will increase much faster and efficiency of nutrient use in agriculture will increase more rapidly in industrialized countries. Adapting Mosaic, with a focus on simple, local solutions, also includes recycling of human urine to produce fertilizers which substitute P fertilizers produced from rock-phosphate and Haber-Bosch-based N fertilizers.

Details on the scenarios in terms of general scenario drivers, and drivers specific to nutrient management in agriculture and urban wastewater trends are provided in Table 7.1.

Table 7.1. Main drivers of ecosystem change for the MEA scenarios from Alcamo et al. (2006) and assumptions for the fertilizer use.

Driver	Global Orchestration (GO)	Order from Strength (OS)	Technogarden (TG)	Adapting Mosaic (AM)
A. General drivers				
Keywords	Globalization, economic development, reactive approach to environmental problems	Regionalization, fragmentation security, reactive approach to environmental problems	Globalization, environmental technology, proactive approach to environmental problems	Regionalization, local ecological management with simple technology, proactive approach to environmental problems
World population	Low	High	Medium	High
(billion)	2000: 6.1	2000: 6.1	2000: 6.1	2000: 6.1
	2030: 7.7	2030: 8.6	2030: 8.2	2030: 8.5
	2050: 8.2	2050: 9.7	2050: 8.9	2050: 9.6
Income	High	Low	High	Medium
(annual per capita GDP growth rate)	2000-2030:2.6% a^{-1}	2000-2030:1.6% a^{-1}	2000-2030:2.1% a^{-1}	2000-2030:1.8% a^{-1}
	2030-2050:3.0% a^{-1}	2030-2050:1.3% a^{-1}	2030-2050:2.6% a^{-1}	2030-2050:2.2% a^{-1}
Global GHG emissions	High	High	Low	Medium
($GtC\text{-}eq\ a^{-1}$)	2000: 9.8	2000: 9.8	2000: 9.8	2000: 9.8
	2050: 25.6	2050: 20.3	2050: 7.1	2050: 18.0
Global mean temperature increase	High	High	Low	Medium
	2000: 0.6	2000: 0.6	2000: 0.6	2000: 0.6
(°C)	2030: 1.4	2030: 1.3	2030: 1.3	2030: 1.4
	2050: 2.0	2050: 1.7	2050: 1.5	2050: 1.9
Per capita food consumption	High, high meat	Low	High, low meat	Low, low meat
Agricultural productivity increase	High	Low	Medium-high	Medium
Energy crops	4% of cropland area	1% of cropland area	28% of cropland area	2% of cropland area

	in 2050	in 2050	in 2050	in 2050
Nutrient use in agriculture				
Fertilizer use and efficiency	No change in countries with a surplus; rapid increase in N and P fertilizer use in countries with soil nutrient depletion (deficit)	No change in countries with a surplus; slow increase in N and P fertilizer use in countries with soil nutrient depletion (deficit)	rapid increase in countries with a surplus; rapid increase in N and P fertilizer use in countries with soil nutrient depletion (deficit)	Moderate increase in countries with a surplus; slow increase in N and P fertilizer use in countries with soil nutrient depletion (deficit); better integration of animal manure and re-cycling of human N and P from households with improved sanitation but lacking a sewage connection.

Table 7.1. Continued.

Driver	Global Orchestration (GO)	Order from Strength (OS)	Technogarden (TG)	Adapting Mosaic (AM)
Urban wastewater				
Urbanization	Downscaling to country scale is from Grübler et al. (2006); B1 is used to represent GO (low urbanization rate), A2r is used for OS (rapid urbanization), B1 for TG (low urbanization rate) and B2 for AM (medium rate).			
Fraction of population with access to improved sanitation	Increase, 2030: reduce 50% of the gap between S_u(2000) and 100% improved sanitation; 2050: reduce 50% of the gap between S_u(2030) and 100% improved sanitation.	Constant 2000 level	Increase as in GO	Constant 2000 level
Fraction of population connected to public sewerage	Increase, 50% of the gap between 2000 level and full connection is closed in the period 2000–2030 and constant afterwards	Constant 2000 level	Increase, As in GO	Constant 2000 level
Detergent use	Laundry detergent use, fraction of P-free laundry detergents, automatic dishwasher detergent use and fraction P-free dishwasher detergents are entirely based on GDP			
Removal of N and P through wastewater treatment plants:	50% of each treatment class shifts toward the next in line[a] in the period 2000–2030 and another 50% in 2030–2050	25% of each treatment class shifts toward the next in line[a] in the period 2000–2030 and another 25% in 2030–2050	As in GO	As in OS

[a] Four treatment classes are distinguished: no treatment (no N or P removal), primary or mechanical treatment (10% N and 10% P removal), secondary or biological treatment (35% N and 45% P removal), and advanced treatment (80% N and 90% P removal). Removal of N and P through wastewater treatment plants will increase by a gradual shift to a higher technological treatment classes. The removal efficiency per class remains constant. In the scenarios 25% (OS and AM) or 50% (GO and TG) of "no treatment" is replaced by mechanical; 25% or 50% of mechanical treatment is replaced by biological; 25% or 50% of biological is replaced by advanced treatment.

Future trends in river nutrient export

DIN export by rivers increased between 1970 and 2000 On all continents (however, to a varying extent); DIN export is projected to further increase in Global Orchestration (Figure 7.4) and decrease in most continents under Adapting Mosaic scenario between 2000 and 2030. The largest changes in DIN export during all time periods and in all scenarios are projected for South Asia.

DIN export in South Asia accounted for 61% (3 Tg) of the global river DIN increase between 1970-2000, and 51% (1.7 Tg) of the global increase during the next 30 years under the Global Orchestration scenario. South America will be responsible for 21% of the global increase according to this scenario. According to the Adapting Mosaic, South Asia will also contribute a major share of the global trend, (54% of the global decrease in DIN river export), followed by Europe (33% of the global decrease) and North America (17%).

There are substantial differences in the relative contributions of various nutrient sources and human drivers causing the scenario trends between developing countries and industrialized countries. Global NEWS scenarios for 2030 and 2050 indicate that substantial changes in coastal nutrient loading may occur due to changing nutrient management in agriculture.

Projected changes vary by nutrient, by nutrient form, and spatially (Figure 7.2 and 7.5). In recent decades some of the largest increases in DIN and DIP loading have occurred in South Asia and South and Central America, and according the Global NEWS scenarios, these regions may well continue to show rapid increases in coastal nutrient loading during the next three to five decades (Figures 7.1-7.3). In all scenarios, South Asia will show the largest increases in DIN export during all time periods; South Asia also shows the largest change in the relative contribution of N sources to DIN export of all the world regions (Figure 7.1). In 1970, the pattern of source contributions was closer to that on the developing countries of South America and Africa. However, by 2000 and in scenarios for 2030 under both Global Orchestration and Adapting Mosaic scenarios, the pattern in South Asia was very similar to that in the industrialized regions Europe and North America, due to the rapid increase in the contribution from fertilizer and manure.

Developing countries in Africa and South America show similar relative contributions of watershed N sources to DIN export in 1970 and 2000 and into the next decades according to Global Orchestration and Adapting Mosaic (Figure 7.1 and 7.3). Biological N_2 fixation in natural ecosystems was the single largest source in 1970, but decreased in importance as anthropogenic sources increase, particularly animal

manure, which by 2030 in both the Global Orchestration and Adapting Mosaic scenarios exceeded the contribution of N_2 fixation in natural ecosystems to DIN export. Nitrogen deposition (natural plus anthropogenic sources) was the third largest contributor to DIN export in all scenarios and all years. Wastewater has not been a major source of river DIN, at the continental scale, for Africa and South America in the past 30 years and is not predicted to be a major source under either scenario in the next 30 years.

Small increases in river DIN export occurred in Europe and North America between 1970 and 2000; according to Global Orchestration DIN export will continue to increase in North America but stabilize in Europe between 2000 and 2030; according to the Adapting Mosaic scenario, DIN export for both continents will decrease by 2030 relative to 2000. The relative contribution of N sources to DIN export across all years and scenarios are similar for Europe and North America (Figure 7.1), with about about equal contributions from natural N_2 fixation, fertilizer, manure, and atmospheric deposition.

An important part of future trends in wastewater discharge are due to differences in population growth (Figure 7.3). In the year 2000 the proportion of inhabitants in both Europe and North America that are connected to a sewage system is high (79% and 70%, respectively). Further increases in connectivity are projected in all scenarios (Figure 7.3), although there is also increased removal efficiency of N in the wastewater treatment facilities. Because the population in Europe is stable, only a slight increase in the wastewater DIN and DIP source is projected (Figure 7.1). However, the population increases somewhat in all MEA scenarios for the U.S.A, and with increasing sewage connection, the wastewater DIN and DIP discharge will slightly increase in all scenarios.

Between 1970 and 2000, the DIP export by rivers increased in all world regions, except for Europe which showed an important decrease and North America with a small decrease (Figure 7.1 and 7.2). DIP export will continue to decrease in Europe between 2000 and 2030, and all other continents showed quite substantial increases according to the Global Orchestration scenario. About 50% of the increase in global river DIP export is in South Asia, while South America and Oceania (17% and 15%, respectively) also account for large part of the global river DIP export increase in Global Orchestration.

The Adapting Mosaic scenario shows less but still substantial increase in DIP river export than under the Global Orchestration for all continents, except again Europe. In the Adapting Mosaic scenario South Asia is responsible for 46% and South America for 27% of the global DIP river export increase relative to 2000.

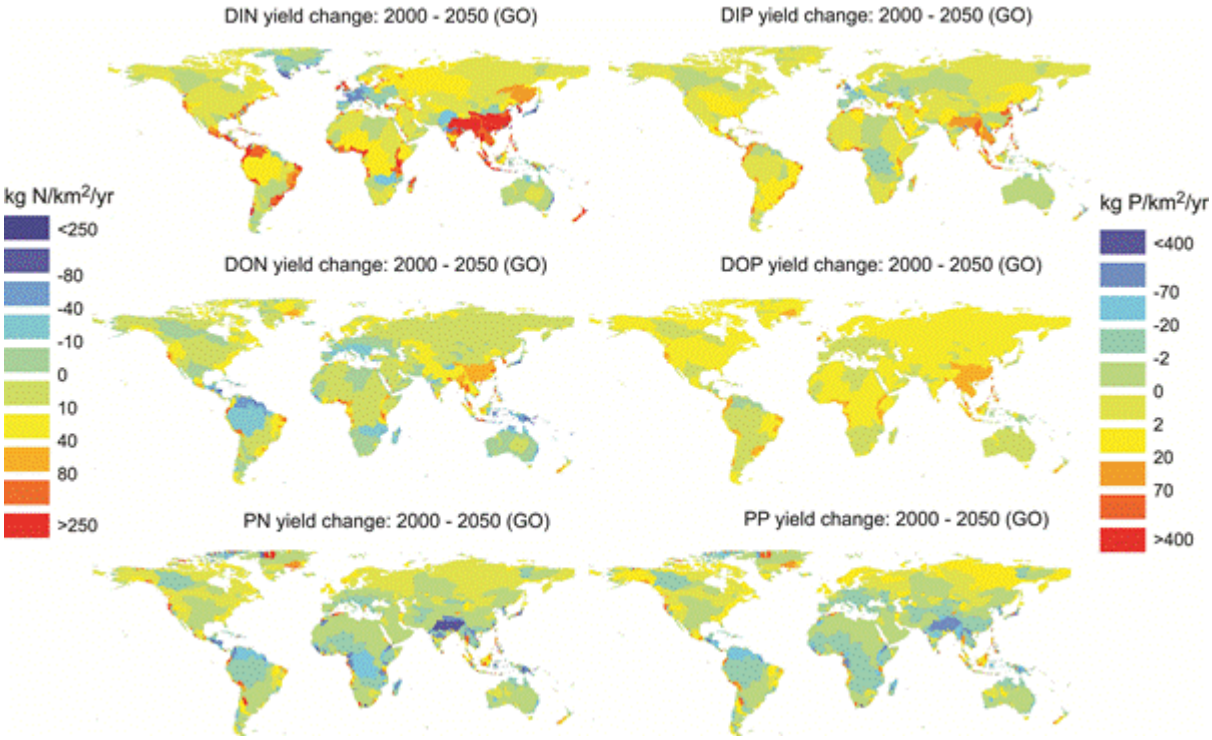

Figure 7.5. Predicted changes in per-area nutrient fluxes by large river basin and nutrient form globally between years 2000 and 2050. Note especially large anticipated changes in DIN and DIP loading in South Asia and parts of Central and South America.

Wastewater was a small nutrient source in the developing countries South Asia, South America and Africa in 1970. In addition to wastewater, manure and detergents were major and growing contributors to DIP export over time in Africa, South America and South Asia. Fertilizer use is also a growing DIP source which in South America and particularly in South Asia will grow at the same rate as wastewater up to 2050. Preventing these dramatic increases in wastewater DIP discharge in regions with fast population growth and fast urbanization is a difficult task for policy makers.

The scenarios for 2050 show major increases in DIN and DIP river export to coastal ecosystems, particularly in South and Eastern Asia, and in many countries in South America and Africa (Figure 7.5). In order to guarantee food security for populations in developing countries, and to prevent land degradation or restore soil fertility, fertilizer use will have to increase. As a consequence, nutrient losses by leaching, volatilization and runoff will inevitably increase. At the same time, urbanization and lagging sewage connection and treatment of wastewater will lead to increasing nutrient discharge to surface water in developing countries. In contrast, important decreasing trends are projected in Europe, and stabilization in North America and Australia. Industrialized countries are assumed to reduce nutrient discharge to rivers by developing improved wastewater treatment systems, and also by reducing ammonia volatilization, leaching and runoff by improved nutrient management.

7.2. Impacts of increased nutrient loading

The above scenarios have been used to analyze potential impacts in coastal marine ecosystems. Relationships developed via work described in the previous chapters were used to develop maps indicating where high chlorophyll *a* concentrations, hypoxia and HABs occur or are likely to occur under current and recent historic conditions, as well as for future scenarios.

Chlorophyll-*a* and Hypoxia

In the course of this project, we discovered that bottom-water O_2 data have recently been made available for much of the world's coastline (Figure 5.1). Similarly, satellite-based estimates of chl *a* concentration provide a reasonable estimate of the location of high chl *a* waters in the coastal zone (Figure 7.6). In addition, the application of primary production models such as the Vertically Generalized Production Model (VGPM (Behrenfeld and Falkowski, 1997)) has facilitated global, spatially explicit estimates of coastal net primary productivity. Hence, instead of using models to in-fill spatial data gaps, we have concentrated on estimating the sensitivity of various coastal systems to potential changes in nutrient loading and physical mixing conditions.

We explored empirical approaches to estimating the effect of nutrient loading and COSCAT physical characteristics on chl *a* concentrations, NPP, and bottom water [O_2], and achieved promising results, suggesting that a large portion of the variation in mean COSCAT [chl a], NPP, and [O_2] can be predicted as a function of coastal physical characteristics and nutrient loading rates (Figure 7.7 a-c). However, mechanistic relationships between independent and dependent variables were not clear, complicating interpretation of model results and the application of such models in a predictive mode. For this reason, we have opted to focus on the more mechanistic COOLBEANS approach (described above in Section 6.2) for coastal hypoxia modeling.

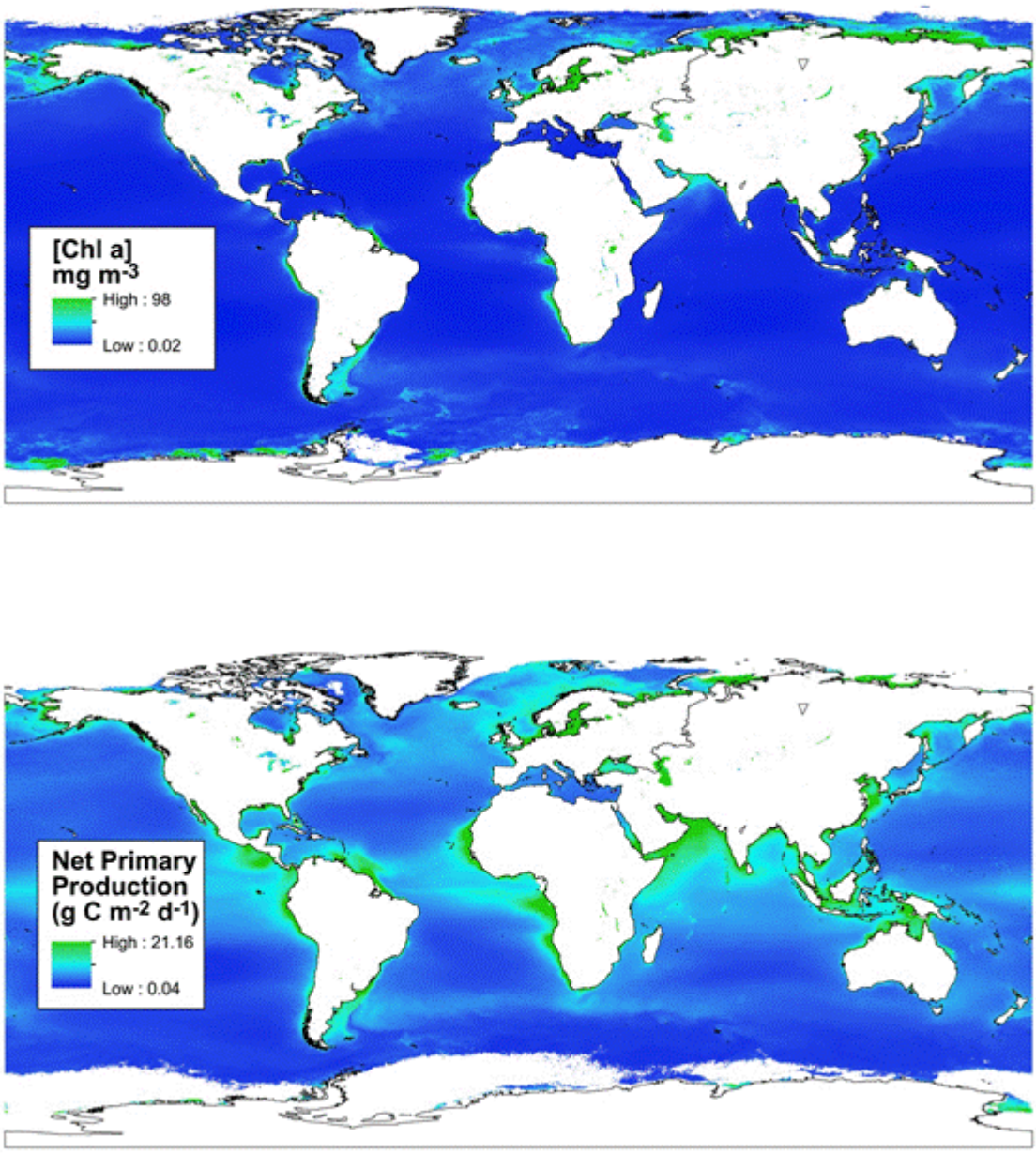

Figure 7.6. MODIS satellite-derived global (a) [chl a] and (b) NPP. NPP was calculated using the Vertically Generalized Production Model (VGPM;(Behrenfeld and Falkowski, 1997)).

Because of this mismatch in scales between localized hypoxia and mean oxygen concentration in COSCATs, it is not judicious to try to reconcile point observations with COSCAT-scale predictions. Nevertheless, comparisons can be made with regions that have experienced expansions in hypoxia that are on a similar scale as the COSCATs that host them, like the Baltic Sea and northern Gulf of Mexico. Predicted hypoxic areas and calculated sensitivities to nutrient loading for these COSCATs are consistent with observations.

COOLBEANS has been used to calculate the sensitivity TO CHANGES IN NUTRIENT LOADING (Figure 7.9). COOLBEANS suggests that O_2 conditions in these regions are likely to be sensitive to additional N inputs. In particular, the west coast of Central America and northern South America, the east coast of the Southeastern Asian peninsula and the east coast of India are indicated as moderately to strongly sensitive to increasing nutrient inputs. To date, relatively few instances of hypoxia have been reported from South Asia or South and Central America (Figure 5.1), but this may change in coming decades as rates of N and P delivery to coastal zones in these regions continue to increase.

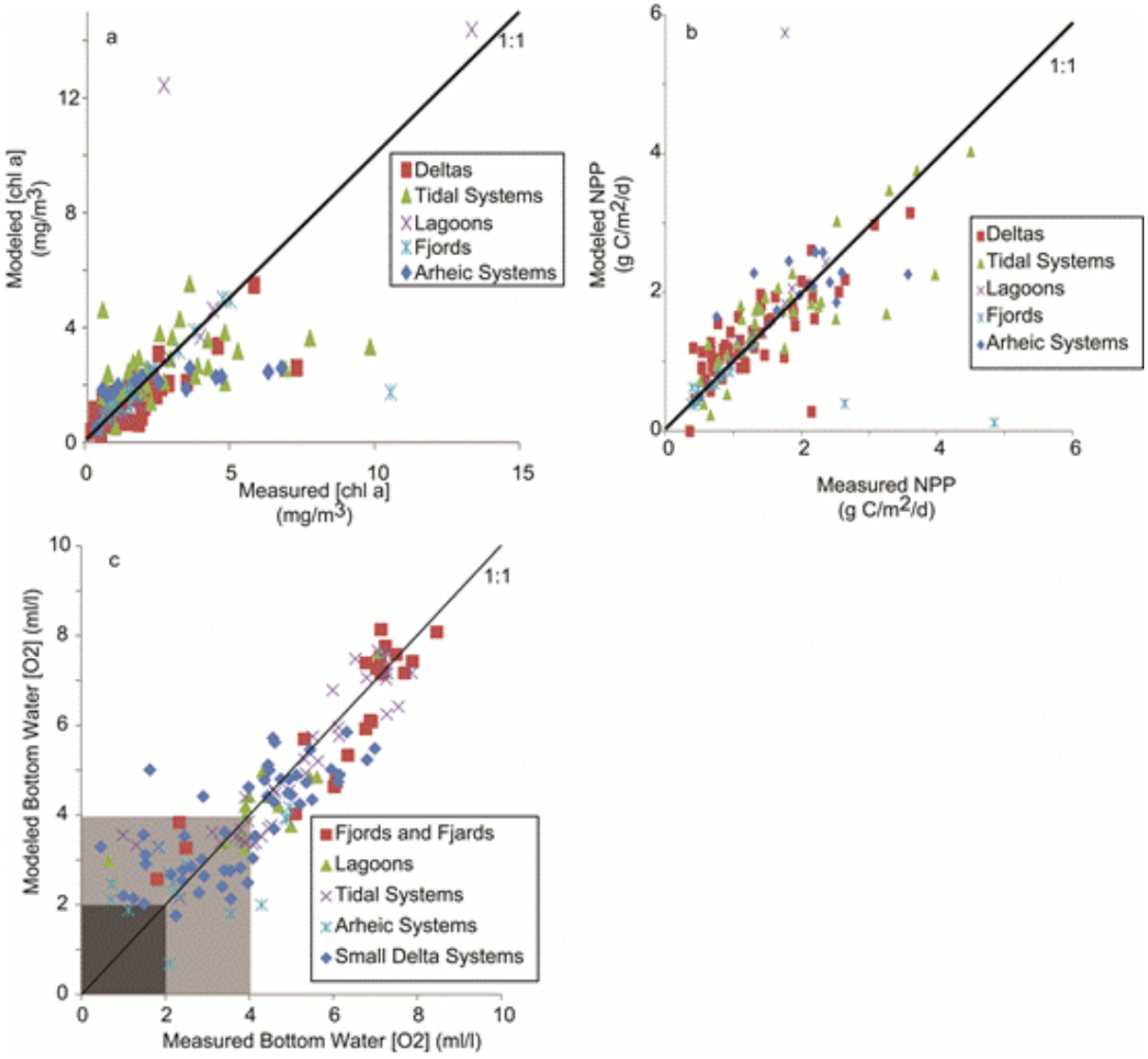

Figure 7.7.. Measured vs predicted (a) [chl a], (b) net primary production, and (c) [O_2] for the world's COSCATs. Individual stepwise multiple regression-based best multiple linear regression models were developed for each of 5 coastal system types using data described in Table 4.1.

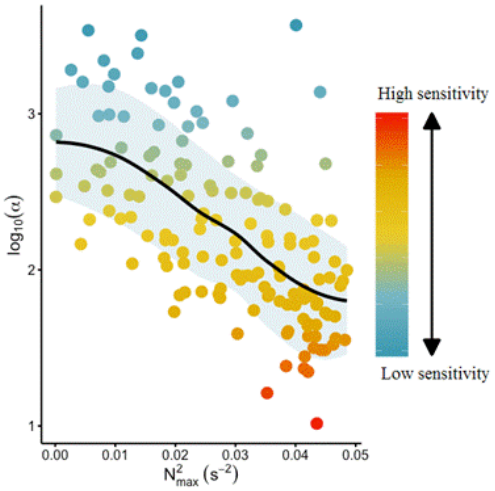

Figure 7.8. Common logarithm of the exchange coefficient between surface and deep waters (Y-axis) versus the maximum buoyancy frequency (X-axis). Color denotes sensitivity to nutrient loading and indicates that this sensitivity increases with stratification.

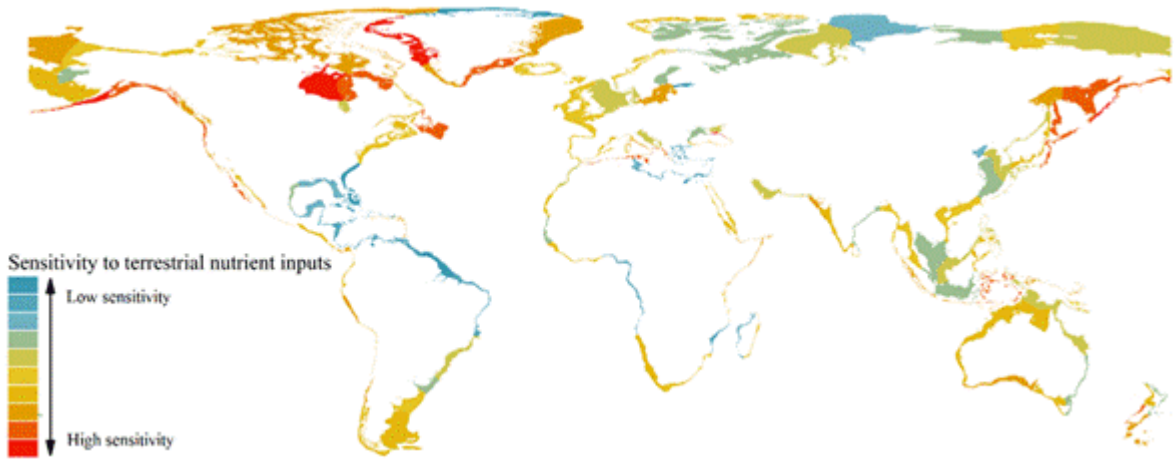

Figure 7.9. Sensitivity of COSCATs to changes in nutrient loading according to COOLBEANS model. Red denotes high sensitivity, whereas blue represents low sensitivity.

Incidences of hypoxia can also be expected to continue in regions where they have already been noted such as around Japan, in the Baltic, and in estuaries along the US coast. In addition to these highlighted regions, there are also a number of regions that appear to be susceptible to nutrient loading-related hypoxia but which are unlikely to experience large increases in nutrient loading over the next several decades due to a lack of land-based human activity (Figure 7.9).

HABs

Between 1970 and 2000 there was a rapid increase in the riverine export of N and P (Seitzinger et al., 2010c). In addition to increases in absolute rates of nutrient loading, there has also been a shift in the ratio of nutrients delivered to coastal zones. Between 1970 and 2000 there has been a distortion of nutrient ratios in many river basins, primarily in large parts of Asia, but also in parts of western part of North America, the eastern part of South America, while the situation, as reflected in ICEP values, improved in parts of Europe, particularly those parts draining to the Baltic, Mediterranean Sea and Black Sea (Figure 7.10). This effect is closely related to the economic collapse of the former Soviet Union and many Eastern European countries.

In coming decades, coastal zones in many world regions are almost certain to see increases in river export of N and P. Meanwhile, Si river export is decreasing globally as a result of eutrophication and retention in the increasing number of reservoirs in the world's river systems. The result of these simultaneous changes of N, P and Si is an increasing ICEP value in many world regions (western part of North America, Eastern part of South America, Africa and Asia, indicating an increasing risk that severe problems associated with eutrophication may occur (Figure 7.10). The number of river basins with positive ICEP values increases in many world regions, as well as the value of ICEP. This increase is greater for rivers draining into the Atlantic Ocean, Indian Ocean and Pacific Ocean (Figure 7.10).

It is worth noting that while changes in Africa were slow between 1970 and 2000, in the coming decades changes in nutrient stoichiometry may be more significant, probably the result of the expected fast population growth and all associated societal and economic changes, such as increasing food and energy production (Section 7.1 and Figure 7.10).

The historical data suggest that HAB risk increased considerably between 1970 and 2000. Scenario results for 2050 indicate that this risk will further spread (South America, Africa) and increase in areas with current high risk (Eastern Asia) (Figure 7.10) There are also large parts of the world where HAB risk is expected to decrease as a result of higher efficiency of nutrient use in agriculture and improved wastewater

treatment. This is particularly so in the Adapting Mosaic scenario, which is a scenario with an orientation towards environmental issues and local simple solutions.

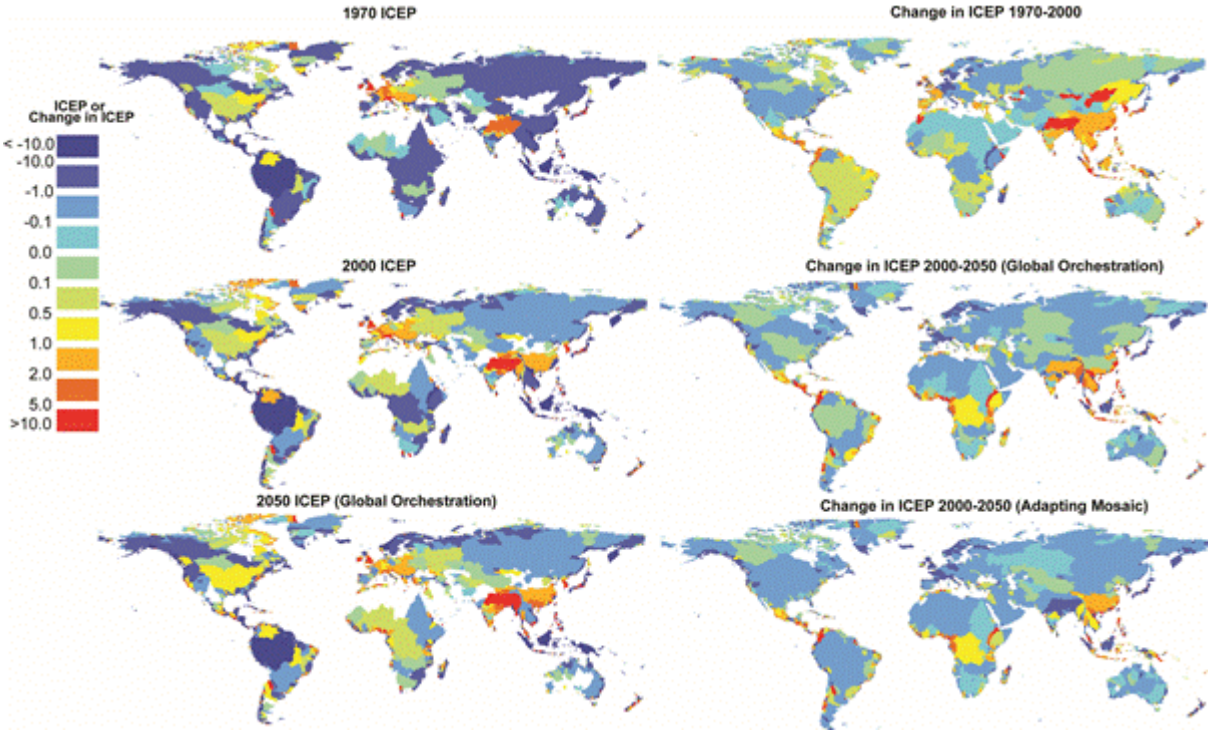

Figure 7.10. Historic and predicted ICEP values and changes in ICEP values by large river basin globally for years 1970, 2000, and 2050. Note especially large anticipated changes in ICEP in South Asia both between 1970 and 2000 and between 2000 and 2050. Note also the contrast between two different development scenarios (Global Orchestration and Adapting Mosaic) in that region of rapid change.

8. Conclusion

Component B of the project GEF project “Global foundations for reducing nutrient enrichment and oxygen depletion from land based pollution, in support of Global Nutrient Cycle” has addressed the need for more quantitative nutrient analysis. In an innovative way, the project has improved predictive capability by developing tools to estimate the magnitude of contributions from various nutrient sources within watersheds and quantitatively analyze relationships between nutrient sources and coastal impacts.

Data were collected on hypoxia events, harmful algal blooms and impacts on fisheries, and these data were used to analyze the impact of the environmental conditions in coastal seas as well as nutrient loading on these events. This project has also generated a unique database on coastal characteristics. This database is the most comprehensive and up-to-date collection of coastal characteristics of which we are aware.

All data presented in this report will be available from the website of the Global Partnership on Nutrient Management (GPNM) (http://www.nutrientchallenge.org/filebrowser). Questions or requests related to this report can be addressed to the authors.

Acknowledgements

Thanks are due to a great number of people. To start with, we are grateful Jan Willem Erisman and Sybil Seitzinger, who initiated this Global Environment Facility (GEF) / United Nations Environment Programme (UNEP) project.

Next we thank all members of the Global NEWS project, in particular Emilio Mayorga for providing help and carefully checking the data and description of the Global NEWS data and Michelle McCrackin for contributing substantially to the enhancement of spatial and temporal resolution of NEWS submodels. Furthermore, Xiaochen Liu collected the Chinese data on harmful algal blooms. We are also grateful to Henrik Enevoldsen for his support during the project.

Literature

Alcamo, J., Van Vuuren, D., and Cramer, W.: Changes in ecosystem services and their drivers across the scenarios, in: Ecosystems and human well-being: Scenarios, edited by: Carpenter, S. R., Pingali, P. L., Bennett, E. M., and Zurek, M. B., Island Press, Washington, D.C., 279-354, 2006.

Anderson, D., M., Gilbert, P. M., and Burkholder, J. M.: Harmful algal blooms and eutrophication: Nutrient sources, composition, and consequences, Estuaries, 25, 704-726, 2002.

Andersson, J. H., Wijsman, J. W. M., Herman, P. M. J., Middleburg, J. J., Soetaert, K., and Heip, C.: Respiration patterns in the deep ocean, Geophysical Research Letters, 31, L03304 03301-03304, 2004.

Behrenfeld, M. J., and Falkowski, P. G.: Photosynthetic rates derived from satellite-based chlorophyll concentration, Limnology and Oceanography, 42, 1-20, 1997.

Behrenfeld, M. J., Boss, E., Siegel, D. A., and Shea, D. M.: Carbon-based ocean productivity and phytoplankton physiology from space, Global Biogeochemical Cycles, 19, Artn Gb1006, 10.1029/2004gb002299, 2005.

Beusen, A. H. W., Dekkers, A. L. M., Bouwman, A. F., Ludwig, W., and Harrison, J.: Estimation of global river transport of sediments and associated particulate c, n, and p, Global Biogeochemical Cycles, 19, GB4S05, 10.1029/2005gb002453, 2005.

Beusen, A. H. W., Bouwman, A. F., Dürr, H. H., Dekkers, A. L. M., and Hartmann, J.: Global patterns of dissolved silica export to the coastal zone: Results from a spatially explicit global model, Global Biogeochemical Cycles, VOL. 23, GB0A02, doi:10.1029/2008GB003281, 2009.

Beusen, A. H. W., Slomp, C. P., and Bouwman, A. F.: Global land–ocean linkage: Direct inputs of nitrogen to coastal waters via submarine groundwater discharge, Environmental Research Letters, 8, 034035, 10.1088/1748-9326/8/3/034035, 2013.

Billen, G., Beusen, A., Bouwman, L., and Garnier, J.: Anthropogenic nitrogen autotrophy and heterotrophy of the world's watersheds: Past, present, and future trends, Global Biogeochemical Cycles, 24, GB0A11, 10.1029/2009gb003702, 2010.

Borsuk, M. E., Higdon, D., Stow, C. A., and Reckhow, K. H.: A bayesian hierarchical model to predict benthic oxygen demand from organic matter loading in estuaries and coastal zones, Ecological Modelling, 143, 165-181, 10.1016/s0304-3800(01)00328-3, 2001.

Bouwman, A. F., Beusen, A. H. W., and Billen, G.: Human alteration of the global nitrogen and phosphorus soil balances for the period 1970–2050, Global Biogeochemical Cycles, 23, GB0A04, 10.1029/2009gb003576, 2009.

Bouwman, A. F., Pawłowski, M., Liu, C., Beusen, A. H. W., Shumway, S. E., Glibert, P. M., and Overbeek, C. C.: Global hindcasts and future projections of coastal nitrogen and phosphorus loads due to shellfish and seaweed aquaculture, Reviews in Fisheries Science, 19, 331-357, 10.1080/10641262.2011.603849, 2011.

Bouwman, A. F., Beusen, A. H. W., Overbeek, C. C., Bureau, D. P., Pawlowski, M., and Glibert, P. M.: Hindcasts and future projections of global inland and coastal nitrogen and phosphorus loads due to finfish aquaculture, Reviews in Fisheries Science, 21, 112-156, 10.1080/10641262.2013.790340, 2013a.

Bouwman, L., Beusen, A., M. Glibert, P. M., Overbeek, C., Pawlowski, M., Herrera, J., Mulsow, S., Yu, R., and Zhou, M.: Mariculture: Significant and expanding cause of coastal nutrient enrichment, Environmental Research Letters, 8, 044026, doi:044010.041088/041748-049326/044028/044024/044026, 2013b.

Breitburg, D. L., Craig, J. K., Fulford, R. S., Rose, K. A., Boynton, W. R., Brady, D. C., Ciotti, B. J., Diaz, R. J., Friedland, K. D., Hagy Iii, J. D., Hart, D. R., Hines, A. H., Houde, E. D., Kolesar, S. E., Nixon, S. W., Rice, J. A., Secor, D. H., and Targett, T. E.: Nutrient enrichment and fisheries exploitation: Interactive effects on estuarine living resources and their management, Hydrobiologia, 629, 31-47, 2009.

Christensen, V., and Walters, C. J.: Trade-offs in ecosystem-scale optimization of fisheries management policies, Bulletin of Marine Science, 74, 549-562, 2004.

Díaz, R. J., Rosenberg, R., Rabalais, N. N., and Levin, L. A.: Dead zone dilemma, Marine Pollution Bulletin, 58, 1767-1768, 10.1016/j.marpolbul.2009.09.030, 2009.

Dumont, E., Harrison, J. A., Kroeze, C., Bakker, E. J., and Seitzinger, S. P.: Global distribution and sources of dissolved inorganic nitrogen export to the coastal zone: Results from a spatially explicit, global model, Global Biogeochemical Cycles, 19, GB4S02, 10.1029/2005gb002488, 2005.

Dürr, H. H., Laruelle, G. G., Van Kempen, C. M., Slomp, C. P., Meybeck, M., and Middelkoop, H.: World-wide typology of near-shore coastal systems: Defining the estuarine filter of river inputs to the ocean, Estuaries and Coasts, 34, 441-458, doi:410.1007/s12237-12011-19381-y, 2011.

Egbert, G. D., and Erofeeva, S. Y.: Efficient inverse modeling of barotropic ocean tides, J. Atmos. Oceanic Technol., 19, 183–204, doi: http://dx.doi.org/10.1175/1520-0426(2002)019<0183:EIMOBO>2.0.CO;2 2002.

FAO: Fishstatj - software for fishery statistical time series [http://www.Fao.Org/fishery/statistics/software/fishstatj/en] (release data march 2013), Fisheries and Aquaculture Information and Statistics Service, Food and Agriculture Organization of the United Nations, Rome, 2013.

Fekete, B. M., Vörösmarty, C. J., and Grabs, W.: High-resolution fields of global runoff combining observed river discharge and simulated water balances, Global Biogeochemical Cycles, 16, 1042, doi 10.1029/1999GB001254, 2002.

Fekete, B. M., Wisser, D., Kroeze, C., Mayorga, E., Bouwman, L., Wollheim, W. M., and Vörösmarty, C.: Millennium ecosystem assessment scenario drivers (1970–2050): Climate and hydrological alterations, Global Biogeochemical Cycles, 24, GB0A12, 10.1029/2009gb003593, 2010.

Garnier, J., Beusen, A., Thieu, V., Billen, G., and Bouwman, L.: N:P:Si nutrient export ratios and ecological consequences in coastal seas evaluated by the icep approach, Global Biogeochemical Cycles, 24, GB0A05, 10.1029/2009gb003583, 2010.

GEOHAB: Global ecology and oceanography of harmful algal blooms, harmful algal blooms in eutrophic systems Unesco Intergovernmental Oceanographic Commission (IOC) and Scientific Committee on Oceanic Research (SCOR), Paris and Baltimore, 74, 2006.

Glibert, P. M., Mayorga, E., and Seitzinger, S.: Prorocentrum minimum tracks anthropogenic nitrogen and phosphorus inputs on a global basis: Application of spatially explicit nutrient export models, Harmful Algae, 8, 33-38, 2008.

Glibert, P. M., Allen, J. I., Bouwman, A. F., Brown, C., Flynn, K. J., Lewitus, A. J., and Madden, C. J.: Modeling of habs and eutrophication: Status, advances, challenges, Journal of Marine Systems, 83, 262-275, 2010.

Gordon, A. L., Sprintall, J., Van Aken, H. M., Susanto, D., Wijffels, S., Molcard, R., Ffield, A., Pranowo, W., and Wirasantosa, S.: The indonesian throughflow during 2004-2006 as observed by the instant program, Dynamics of Atmospheres and Oceans, 50, 115-128, 2010.

Grübler, A., O'Neill, B., Riahi, K., Chirkov, V., Goujon, A., Kolp, P., Prommer, I., Scherbov, S., and Slentoe, E.: Regional, national, and spatially explicit scenarios of demographic and economic change based on sres, Environment Science and Technology, doi:10.1016/j.techfore.2006.05.023, 2006.

Harrison, J. A., Caraco, N., and Seitzinger, S. P.: Global patterns and sources of dissolved organic matter export to the coastal zone: Results from a spatially explicit, global model, Global Biogeochemical Cycles, 19, GB4S04, 10.1029/2005gb002480, 2005a.

Harrison, J. A., Seitzinger, S. P., Bouwman, A. F., Caraco, N. F., Beusen, A. H. W., and Vörösmarty, C. J.: Dissolved inorganic phosphorus export to the coastal zone: Results from a spatially explicit, global model, Global Biogeochemical Cycles, 19, GB4S03, 10.1029/2004gb002357, 2005b.

Harrison, J. A., Bouwman, A. F., Mayorga, E., and Seitzinger, S.: Magnitudes and sources of dissolved inorganic phosphorus inputs to surface fresh waters and the coastal zone: A new global model, Global Biogeochemical Cycles, 24, GB1003, 10.1029/2009gb003590, 2010a.

Harrison, J. A., Bouwman, A. F., Mayorga, E., and Seitzinger, S.: Magnitudes and sources of dissolved inorganic phosphorus inputs to surface fresh waters and the coastal zone: A new global model, Global Biogeochem Cycles, 24, GB1003, doi:10.1029/2009GB003590, 2010b.

Lamarque, J. F., Dentener, F., McConnell, J., Ro, C. U., Shaw, M., Vet, R., Bergmann, D., Cameron-Smith, P., Dalsoren, S., Doherty, R., Faluvegi, G., Ghan, S. J., Josse, B., Lee, Y. H., MacKenzie, I. A., Plummer, D., Shindell, D. T., Skeie, R. B., Stevenson, D. S., Strode, S., Zeng, G., Curran, M., Dahl-Jensen, D., Das, S., Fritzsche, D., and Nolan, M.: Multi-model mean nitrogen and sulfur deposition from the atmospheric chemistry and climate model intercomparison project (accmip): Evaluation of historical and projected future changes, Atmos. Chem. Phys., 13, 7997-8018, 10.5194/acp-13-7997-2013, 2013.

Laruelle, G. G., Dürr, H. H., Lauerwald, R., Hartmann, J., Slomp, C. P., Goossens, N., and Regnier, P. A. G.: Global multi-scale segmentation of continental and coastal waters from the watersheds to the continental margins, Hydrology and Earth System Sciences, 17, 2029-2051, 2013.

Lehner, B., and Döll, P.: Development and validation of a global database of lakes, reservoirs and wetlands, Journal of Hydrology, 296, 1-22, 2004.

Lim, H.-S., Diaz, R. J., Hong, J.-S., and Schaffner, L. C.: Hypoxia and benthic community recovery in korean coastal waters,, Marine Pollution Bulletin, 52, 1517-1526, doi:1510.1016/j.marpolbul.2006.1505.1013., 2006.

Ludwig, W., Bouwman, A. F., Dumont, E., and Lespinas, F.: Water and nutrient fluxes from major mediterranean and black sea rivers: Past and future trends and their implications for the basin-scale budgets, Global Biogeochemical Cycles, 24, GB0A13, 10.1029/2009gb003594, 2010.

Mayorga, E., Seitzinger, S. P., Harrison, J. A., Dumont, E., Beusen, A. H. W., Bouwman, A. F., Fekete, B. M., Kroeze, C., and Van Drecht, G.: Global nutrient export from watersheds 2 (news 2): Model development and implementation, Environmental Modelling and Software, 25, 837-853, 2010.

McCrackin, M. L., Harrison, J. A., and Compton, J. E.: A comparison of news and sparrow models to understand sources of nitrogen delivered to us coastal areas, Biogeochemistry, 114, 281-297, 10.1007/s10533-012-9809-x, 2013.

McCrackin, M. L., Harrison, J. A., and Compton, J. E.: Factors influencing export of dissolved inorganic nitrogen by major rivers: A new, seasonal, spatially explicit, global model, Global Biogeochemical Cycles, 28, 269-285, 10.1002/2013gb004723, 2014.

McCrackin, M. L., Harrison, J. A., and Compton, J. E.: Future riverine nitrogen export to coastal regions in the united states: Prospects for improving water quality, Journal of Environmental Quality, 44, 345-355, 10.2134/jeq2014.02.0081, 2015.

Meybeck, M.: Carbon, nitrogen and phosphorous transport by world rivers, American Journal of Science, 282, 401-450, 1982.

Middelburg, J. J., Soetaert, K., and Herman, P. M. J.: Empirical relationships for use in global diagenetic models, Deep-Sea Research Part I: Oceanographic Research Papers, 44, 327-344, 10.1016/s0967-0637(96)00101-x, 1997.

Middelburg, J. J., and Levin, L. A.: Coastal hypoxia and sediment biogeochemistry, Biogeosciences, 6, 1273-1293, 10.5194/bg-6-1273-2009, 2009.

Nixon, S. W., and Buckley, B. A.: "A strikingly rich zone" - nutrient enrichment and secondary production in coastal marine ecosystems, Estuaries, 25, 782-796, Doi 10.1007/Bf02804905, 2002.

NOAA: World ocean atlas 2009 (https://www.Nodc.Noaa.Gov/oc5/woa09/pr_woa09.Html), accessed 2014, 2009.

Rabalais, N. N.: Nitrogen in aquatic ecosystems, Ambio, 31, 102-112, 2002.

Redfield, A. C., Ketchum, B. H., and Richards, F. A.: The influence of organisms on the composition of sea-water, in: The sea, edited by: Hills, M. N., Wiley and Sons, New York, 12-37, 1963.

Rousseau, V., Becquevort, S., Parent, J.-Y., Gasparini, S., Daro, M.-H., Tackx, M., and Lancelot, C.: Trophic efficiency of the planktonic food web in a coastal ecosystem dominated by phaeocystis colonies, Journal of Sea Research, 43, 357-372, doi:310.1016/S1385-1101(1000)00018-00016, 2000.

Seitzinger, S. P., Harrison, J. A., Dumont, E., Beusen, A. H. W., and Bouwman, A. F.: Sources and delivery of carbon, nitrogen, and phosphorus to the coastal zone: An overview of global nutrient export from watersheds (news) models and their application, Global Biogeochemical Cycles, 19, GB4S01, 10.1029/2005gb002606, 2005.

Seitzinger, S. P., Bouwman, A. F., and Kroeze, C.: Preface to special section on past and future trends in nutrient export from global watersheds and impacts on water quality and eutrophication, Global Biogeochemical Cycles, 24, GB0A01, 10.1029/2010gb003851, 2010a.

Seitzinger, S. P., Mayorga, E., Bouwman, A. F., Kroeze, C., Beusen, A. H. W., Billen, G., Van Drecht, G., Dumont, E., Fekete, B. M., Garnier, J., Harrison, J., Wisser, D., and Wollheim, W. M.: Global river nutrient export: A scenario analysis of past and future trends, Glob Biogeochem Cycles, 24, GB0A08, doi:10.1029/2009GB003587, 2010b.

Seitzinger, S. P., Mayorga, E., Bouwman, A. F., Kroeze, C., Beusen, A. H. W., Billen, G., Van Drecht, G., Dumont, E., Fekete, B. M., Garnier, J., and Harrison, J. A.: Global river nutrient export: A scenario analysis of past and future trends, Global Biogeochemical Cycles, 24, GB0A08, 10.1029/2009gb003587, 2010c.

State oceanic administration chinapeople's republic. Http://www.Soa.Gov.Cn/zwgk/hygb/zghyzhgb/ (in chinese), 2014.

Soetaert, K., Herman, P. M. J., and Middelburg, J. J.: A model of early diagenetic processes from the shelf to abyssal depths, Gechimica et Cosmochimica Acta, 60, 1019-1040, 1996.

Thieu, V., Mayorga, E., Billen, G., and Garnier, J.: Subregional and downscaled global scenarios of nutrient transfer in river basins: Seine-somme-scheldt case study, Global Biogeochemical Cycles, 24, GB0A10, 10.1029/2009gb003561, 2010.

van der Struijk, L. F., and Kroeze, C.: Future trends in nutrient export to the coastal waters of south america: Implications for occurrence of eutrophication, Global Biogeochemical Cycles, 24, GB0A09, 10.1029/2009gb003572, 2010.

Van Drecht, G., Bouwman, A. F., Boyer, E. W., Green, P., and Siebert, S.: A comparison of global spatial distributions of nitrogen inputs for nonpoint sources and effects on river nitrogen export, Global Biogeochemical Cycles, 19, GB4S06, 10.1029/2005gb002454, 2005.

Van Drecht, G., Bouwman, A. F., Harrison, J., and Knoop, J. M.: Global nitrogen and phosphate in urban wastewater for the period 1970 to 2050, Global Biogeochemical Cycles, 23, GB0A03, 10.1029/2009gb003458, 2009.

Yan, W., Mayorga, E., Li, X., Seitzinger, S. P., and Bouwman, A. F.: Increasing anthropogenic nitrogen inputs and riverine din exports from the changjiang river basin under changing human pressures, Global Biogeochemical Cycles, 24, GB0A06, 10.1029/2009gb003575, 2010.

Yasin, J. A., Kroeze, C., and Mayorga, E.: Nutrients export by rivers to the coastal waters of africa: Past and future trends, Global Biogeochemical Cycles, 24, GB0A07, 10.1029/2009gb003568, 2010.